The Report Committee for Sriram Chandrasekhar
Certifies that this is the approved version of the following report:

Wettability Alteration with Brine Composition in High Temperature Carbonate Reservoirs

APPROVED BY
SUPERVISING COMMITTEE:

Supervisor:

Kishore K. Mohanty

Larry W. Lake

Wettability Alteration with Brine Composition in High Temperature Carbonate Reservoirs

by

Sriram Chandrasekhar, BSChE

Report

Presented to the Faculty of the Graduate School of

The University of Texas at Austin

in Partial Fulfillment

of the Requirements

for the Degree of

Master of Science in Engineering

The University of Texas at Austin

August 2013

Dedication

To my ever-supportive parents.

Acknowledgements

I would like to express my sincere gratitude to Dr. Kishore K. Mohanty for his patience, guidance, insight and invaluable time spent on discussions. I am truly privileged to study under him. I am also thankful to Dr. Larry W. Lake for reading and providing valuable feedback on this report.

I would like to thank several people at the Petroleum & Geosystems Engineering Department. Thanks to Dr. Kamy Sepehrnoori for academic advice, Frankie Hart for administrative help, Gary Miscoe and Glen Baum for technical help, and Roger Terzian for computer upgrades and support. I thank Barbara Messmore for assistance, administrative support and pleasant conversations to lift up spirits. Specific thanks and gratitude go to Dr. Eric K. Dao for helping me through this research work offering advice, conversation, manual labor and laughs.

I am deeply appreciative of my colleagues from the Mohanty research group for their friendship, advice and suggestions including Peila Chen, Gaurav Sharma, Himanshu Sharma and many others. I would also like to thank several of my good friends who offered much needed companionship as we completed the program.

I acknowledge the sponsor of this project for providing field resources and making this work possible. Finally, I sincerely thank my incredible parents for unwavering support and belief in me.

Abstract

Wettability Alteration with Brine Composition in High Temperature Carbonate Reservoirs

Sriram Chandrasekhar, M.S.E.

The University of Texas at Austin, 2013

Supervisor: Kishore K. Mohanty

The effect of brine ionic composition on oil recovery was studied for a limestone reservoir rock at a high temperature. Contact angle, imbibition, core flood and ion analysis were used to find the brines that improve oil recovery and the associated mechanisms. Contact angle experiments showed that modified seawater containing Mg^{2+} and SO_4^{2-} and diluted seawater change aged oil-wet calcite plates to more water-wet conditions. Seawater with Ca^{2+}, but without Mg^{2+} or SO_4^{2-} was unsuccessful in changing calcite wettability. Modified seawater containing Mg^{2+} and SO_4^{2-}, and diluted seawater spontaneously imbibe into the originally oil-wet limestone cores. Modified seawater containing extra SO_4^{2-} and diluted seawater improve oil recovery from 40% OOIP (for formation brine waterflood) to about 80% OOIP in both secondary and tertiary modes. The residual oil saturation to modified brine injection is approximately 20%. Multi ion exchange and mineral dissolution are responsible for desorption of organic acid groups which lead to more water-wet conditions. Further research is needed for scale-up of these mechanisms from cores to reservoirs.

Table of Contents

List of Tables

List of Figures

Chapter 1: Introduction

1.1 MOTIVATION

In 2013, the world's proven oil reserves were estimated at 1600 billion barrels of oil and approximately 40-45% is located in carbonate reservoirs (OPEC, 2013; BP, 2013, Schlumberger, 2007) under harsh conditions of high temperatures >100^{o}C and high salinity >100,000 ppm total dissolved solids (TDS). Traditional recovery methods involve primary production by reservoir pressure depletion followed by secondary production, e.g. water flooding which leaves behind a large residual oil saturation of 60-70%. The water flood recovery is low because carbonate reservoirs are characteristically mixed-wet to oil-wet and heterogeneous with low permeability; these properties give low oil relative permeability and allow un-swept zones. Reversing the rock wettability to a water-wet state can reduce these effects and give significantly improved oil recovery from a number of formations.

Several methods for enhanced oil recovery (EOR) have been explored in the last 60 years including chemical injection. However, harsh reservoir conditions limit the use of surfactant-polymer flooding; many surfactants and polymers are unstable at high temperatures and salinities, and low permeability rock constrains polymer transport. The high level of heterogeneity in carbonate reservoirs deteriorates gas injection recovery methods. In this report, the ion composition and salinity of injection water is studied for any wettability altering ability. Advantages to finding a successful brine formulation includes little to no changes in field water injection apparatus, producing more oil with current operating and capital costs compared to chemical or gas based EOR. Brine composition and salinity effects have been extensively studied in sandstones for many

years identifying potential mechanisms behind increased oil recovery. These principles are now gaining traction and being extended to carbonate studies.

The main reservoir considered is a low permeability (50 millidarcy and less) rock composed of limestone with a negligible fraction of dolomite at 120^{o}C. The formation brine salinity is 180,000 ppm TDS, close to saturation by calcium ions. The oil is light (API 40) and contains organic acids that play a major role in creating the oil-wet state of the carbonate rock.

The goal of this study is to identify the brine compositions that can change the wetting state of the oil saturated rock from oil-wet to water-wet, reducing oil trapping and lowering the residual oil saturation to water flooding. Candidate brines were screened by contact angle studies, spontaneous imbibition and core flood experiments. The study is designed to deliver insights into the behavior of ions and the mechanisms behind wettability alteration.

1.2 OUTLINE

This chapter introduced the topic and described the objective of the report. Chapter 2 gives definitions and background of relevant petroleum engineering concepts used in this work and includes a literature review of the subject. Chapter 3 details the experimental material, equipment and procedures used. The results are presented and discussed in chapter 4, and chapter 5 lists the conclusions drawn from this study supplemented with recommendations for future work.

Chapter 2: Background & Literature Review

This chapter defines and discusses wettability and mechanisms of wettability alteration. A survey of relevant literature on low salinity brine triggered enhanced oil recovery is presented, identifying postulated mechanisms and governing parameters.

2.1 Overview

Routine oil recovery technology (primary and secondary) can economically recover around 30-40% of reservoir oil. Primary production uses the reservoir's natural forces to push oil to the surface, but these natural pressures decrease with production requiring secondary recovery methods that involve fluid injection. Waterflooding is popular, but other industry relevant methods include gas injection (to maintain reservoir pressure or as a means to increase wellbore flow rates) with produced natural gas. Reservoir heterogeneity, wettability and capillary forces are three properties that limit the recovery efficiency of these standard methods. Enhanced oil recovery (EOR) techniques look at ways to counter one or more of these undesirable properties to recover more oil.

EOR is oil recovery by the injection of materials not normally present in the reservoir (Lake, 1989) and can be applied in the secondary or tertiary mode. It can be split into four areas: thermal, gas, chemical and others. Thermal methods include in-situ combustion, electrical heating, injection of steam or hot water, and target oil viscosity reduction to improve its mobility. Gas methods inject carbon dioxide, light hydrocarbons, flue gas or nitrogen at pressures where the gas is either miscible or immiscible with the oil. In 2012, there were 62 thermal projects and 141 gas projects ongoing in the United States, accounting for most of the EOR production (Oil and Gas Journal, 2012). Chemical methods involve injection of water miscible surfactants, polymers, alkali and co-solvents. Single chemicals or combinations can target macroscopic sweep efficiency by use of

polymer to block high permeability zones, capillary trapping with surfactants that allow low interfacial tension between oil and brine, and/or rock wettability depending on the system studied. Other EOR methods include use of microbes or enzymes that can break down oil molecules; viscous oils may be degraded to more mobile components, perhaps changing wettability and interfacial tension in the process. Economics and engineering analysis dictate which application would best suit a particular field since tertiary recovery modes typically add to the overall cost of the project above primary and secondary mode costs.

	2012
Thermal	
Steam	48
In situ combustion	12
Hot water	2
Total	62
Gas/Solvent	
HC miscible	12
HC immiscible	1
CO2 miscible	112
CO2 immiscible	9
Nitrogen	3
Total	141
Chemical	
Alkali/Surfactant/Polymer	3
Total	3

Table 2-1: Active domestic EOR projects (Oil and Gas Journal, 2012)

The study of low salinity flooding of sandstone and carbonate rock as an EOR method began 60 years ago and has become a hot topic in the last decade. This report examines wettability alteration of a limestone rock, from oil-wet to water-wet state, by low salinity flooding, analyzing publications for insight about mechanisms behind

improved oil recovery. This change in wettability is expected to reduce capillary trapping effects and marginally improve microscopic sweep.

2.2 WETTABILITY

2.2.1 Definition

Wettability is a solid surface's preference for one fluid over another immiscible fluid. In three phase systems, there are three interfaces (oil-water, water-solid, oil-solid) as indicated in Figure 2-1, with three interfacial tensions (σ_{ij}), and an angle between the two fluid phases (contact angle, θ) measured through the denser phase.

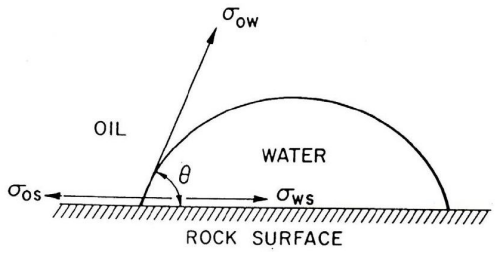

Figure 2-1: Water-oil-rock system exhibiting water-wet contact angle (Peters, 2012)

At equilibrium, the interfacial tensions (IFT) are related by Young's equation, obtained by a force balance:

$$\sigma_{os} - \sigma_{ws} = \sigma_{ow} cos\theta \qquad (2\text{-}1)$$

where, σ_{os} is the solid-oil IFT, σ_{ws} is the solid-water IFT, and σ_{ow} is the water-oil IFT. For the water-oil-rock system, the contact angle is measured through the water phase. There are four wettability states that give rise to drops with different contact angles: Figure 2-2a shows $\theta > 0^o$ indicating an oil-wet solid surface with $\sigma_{ws} > \sigma_{ow} + \sigma_{os}$; Figure 2-2b shows $\theta = 90^o$ indicating a neutral-wet solid surface with $\sigma_{ws} = \sigma_{os}$; Figure 2-2c shows $\theta < 90^o$ indicating a water-wet solid surface with $\sigma_{os} > \sigma_{ow} + \sigma_{ws}$; Figure 2-2d shows $\theta = 0^o$ indicating perfect water-wetting. A perfectly oil-wet surface would give $\theta = 180^o$.

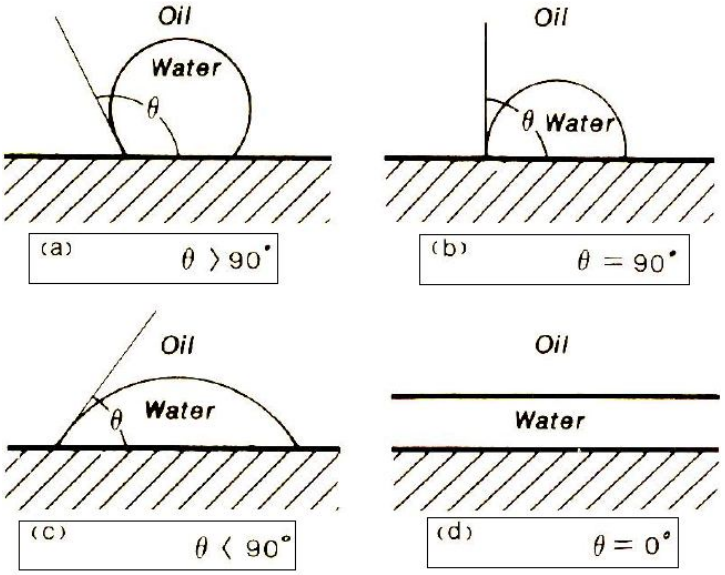

Figure 2-2: Equilibrium contact angles showing four wettability states (Peters, 2012)

In application to petroleum reservoirs, the local wettability strongly influences the distribution, orientation and flow of fluids in porous media (Morrow, 1990). The classification of wetting state is somewhat relaxed when interpreting contact angles in practice: contact angles from 0 to 75^{o} are considered water-wet, 75 to 105^{o} are neutral-wet or intermediate-wet, and 105 to 180^{o} are oil-wet. Salathiel (1973) introduced the concept of mixed wettability in a reservoir where the four types of wettability can occur in different locations of the same reservoir giving different fluid arrangements.

Figure 2-3 indicates the fluid distribution in different wetting states; Figure 2-3A shows a water-wet case where brine coats the surface and is continuous through pore throats while oil is found as large droplets in the center of pore spaces and are disconnected; Figure 2-3C shows an oil-wet surface where the opposite of the water-wet system is true and the oil phase is connected. Figure 2-3B shows a mixed wet surface and indicates certain sections of oil-wet fluid distribution and other sections of water-wet fluid distribution. Salathiel (1973) suggested that in the mixed-wet case, the oil occupies

the large pore spaces and wets the rock, while water occupies the small pores and in turn wets them.

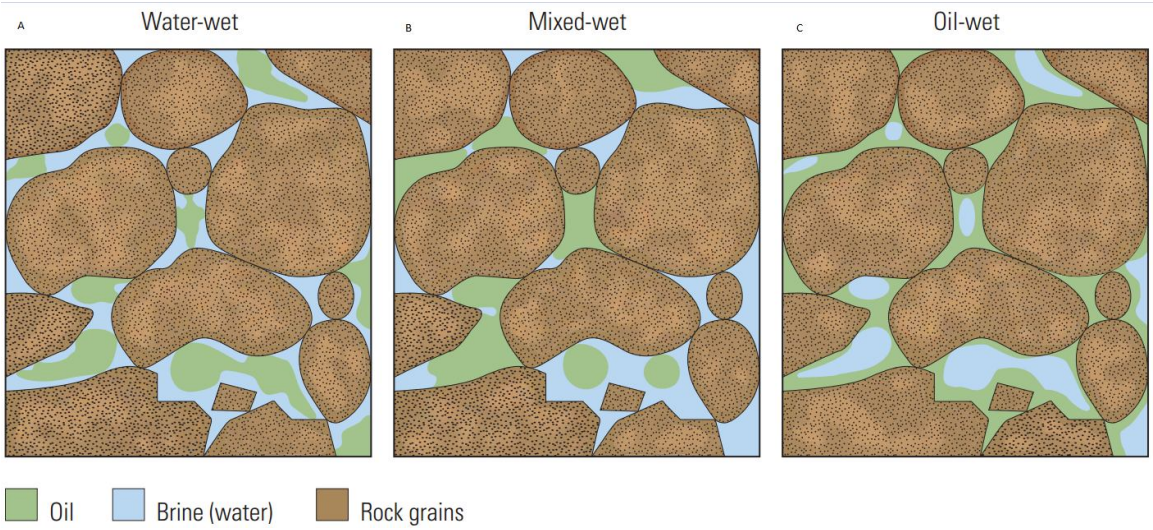

Figure 2-3: Wetting in pores for similar saturations (Abdullah et al., 2007)

2.2.2 Measuring Wettability

There are simple and quick qualitative ways to measure the wettability that involve visually inspecting the arrangement of fluids on a solid sample. Wettability effects can also be seen in derived rock properties in flow experiments, such as the capillary pressure curve or relative permeability behavior. Anderson (1986b) extensively reviews the methods listed in Table 2-2. The contact angle and Amott quantitative methods are considered in this study. Some methods cannot be conducted at exact reservoir conditions of high temperature and pressure.

Qualitative	Condition	
	T	P
Microscopic examination	L	L
Glass slide	H	L
Spontaneous Imbibition	H	L
Flotation	H	L
Capillary pressure curve	H	H
Relative permeability	H	H
Electrical resistivity	H	H

Quantitative	Condition	
	T	P
Contact angle	H	L
Amott	L	H
USBM	L	H
Amott-USBM	L	H

Table 2-2: List of some qualitative and quantitative methods to measure wettability

2.2.2.1 Contact Angle

This method measures the contact angle between a solid surface and the fluids being studied, as partially introduced in section 2.2.1. These experiments require a perfectly smooth solid surface to view contact angles otherwise incorrect values can be measured ($\theta_{apparent}$ vs. θ_{true} in Figure 2-4A). Reservoir rock is porous and has asperities that can influence fluid film thickness giving artificial wettability estimates, and difficult to polish to a smooth surface. Pure mineral crystals that simulate the rock pore wall material are used instead, e.g., sandstone is substituted with quartz crystal and limestone is substituted with calcite crystal.

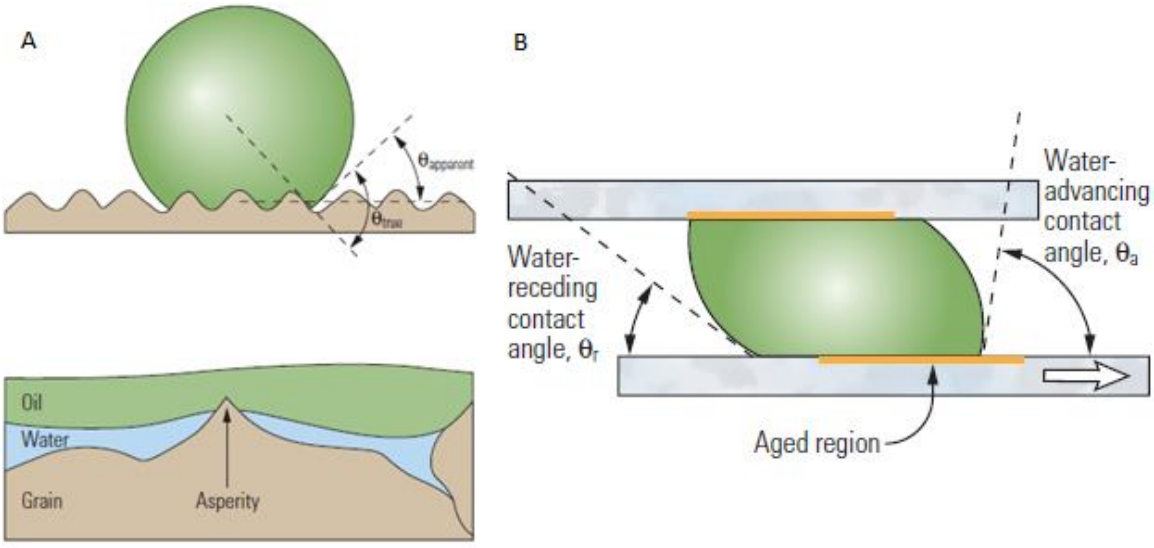

Figure 2-4: A) Pore surface roughness influencing contact angle view; B) Advancing and receding contact angles (Abdullah et al., 2007)

The contact angle measured can also vary with the direction of interface movement. The advancing contact angle is seen when water comes into equilibrium with a surface previously in contact with oil (Figure 2-4B), while the receding contact angle is seen when oil comes into equilibrium with a surface previously contacted by water. The advancing contact angle applies to the in situ water flooding process of an oil-filled reservoir rock.

2.2.2.2 Amott-Harvey Test

This is an imbibition-based method to measure the wettability of a core. The principle is that the wetting fluid will spontaneously imbibe into a core and displace the non-wetting fluid. The experiment begins with a restored state core sample at irreducible water saturation (S_{wirr}) and high initial oil saturation.

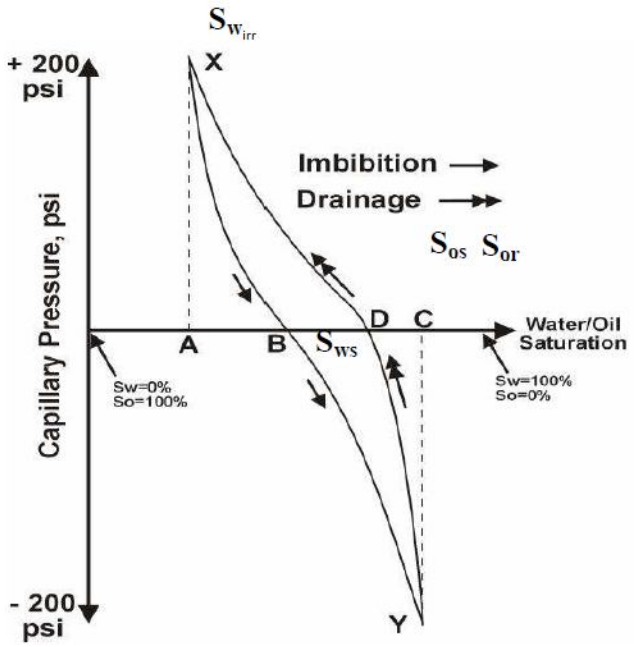

Figure 2-5: Annotation of Amott-Harvey test procedure

1) The core is placed in an imbibition cell to spontaneously imbibe water over a period of time shown by curve, measuring the oil recovery (AB in Figure 2-5).

2) The sample is then centrifuged to force more water in, noting down oil recovery (BC).

3) The sample is now at residual oil saturation (S_{or}) and placed in an imbibition cell to spontaneously imbibe oil, noting the water recovery (CD).

4) Oil is now forced in, to note the final water recovery (AD).

Whichever fluid showed the least recovery indicates the wetting state. The Amott-Harvey index is calculated as follows (see Anderson, 1986b for full details):

$$I_{A-H} = I_w - I_o \tag{2-2}$$

$$I_w = \frac{S_{ws} - S_{wirr}}{S_{wf} - S_{wirr}} = \frac{AB}{AC} = \frac{AB}{AB + BC} \tag{2-3}$$

$$I_o = \frac{S_{os} - S_{or}}{S_{of} - S_{or}} = \frac{CD}{AC} = \frac{CD}{AB + BC} \tag{2-4}$$

If the spontaneous imbibition of water is greater than the imbibition of oil then I_w will be greater than I_o and the Amott-Harvey Index, I_{A-H}, is positive. The index can vary from +1 (completely water-wet) to -1 (completely oil-wet). The exact classification can be somewhat relaxed to allow for experimental error, similar to the contact angle classification.

2.2.3 Wettability - Fundamental View

It is useful to review the theory behind the contact angle further since it is governed by intermolecular forces that are functions of the ions in the brine, oil and mineral surface, the variables this study looks to control. The material is sourced from Hirasaki (1991), an excellent review of the subject.

2.2.3.1 Thermodynamics of Wettability

A more accurate view of the contact angle in a three-phase system is given in Figure 2-6, which shows the wetting phase extending between the non-wetting phase and mineral surface as a thin film. In this region, the film is bounded by two interfaces (mineral/water and water/oil) and the film thickness (h) is the dependent thermodynamic variable. The disjoining pressure is the force per unit area that tends to disjoin or separate the two interfaces.

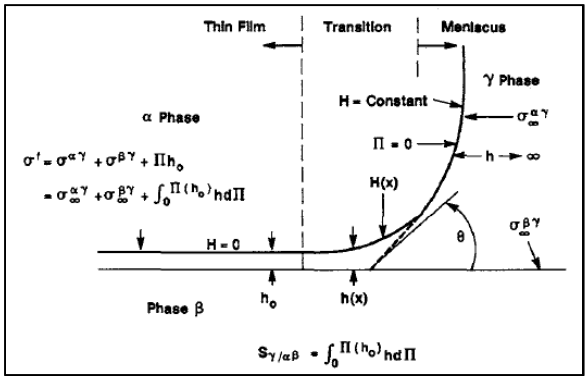

Figure 2-6: Contact region between two fluids and a solid (Hirasaki, 1991)

The conditions for equilibrium in this case are equality of temperature and chemical potentials between the phases, and the augmented Young-Laplace equation,

$$p^{\alpha} - p^{\gamma} = \Pi + 2H^{\alpha\gamma}\sigma^{\alpha\gamma} \qquad (2\text{-}5)$$

where $H^{\alpha\gamma}$=mean curvature, $\sigma^{\alpha\gamma}$=mean IFT, and p^{α}-p^{γ}=capillary pressure, P_c. In the meniscus region, the disjoining pressure is Π=0 giving the Young-Laplace equation. The disjoining pressure can be related to a free-energy function or interaction potential that is zero in the equilibrium configuration.

2.2.3.2 Contact Angle and Film Stability

The contact angle is found when extrapolating the macroscopic meniscus to zero thickness (Figure 2-7). An alternative to Young's equation (2-1) is to integrate equation (2-5) with the curvature expression substituted in. The resulting equation relates the angle of inclination, α, to the specific interaction potential, where angle increases or decreases identify the concave and convex regions of the microscopic meniscus. Along the meniscus, Π=0 and the equation gives the macroscopic contact angle, θ. The interaction potential versus film thickness function is a complex function demonstrating maxima and minima, which in turn creates hysteresis in the contact angle depending on whether the system is formed by thinning from a large separation or if the film is formed by adsorption from zero thickness. This is the basis for the difference between the advancing and receding contact angles.

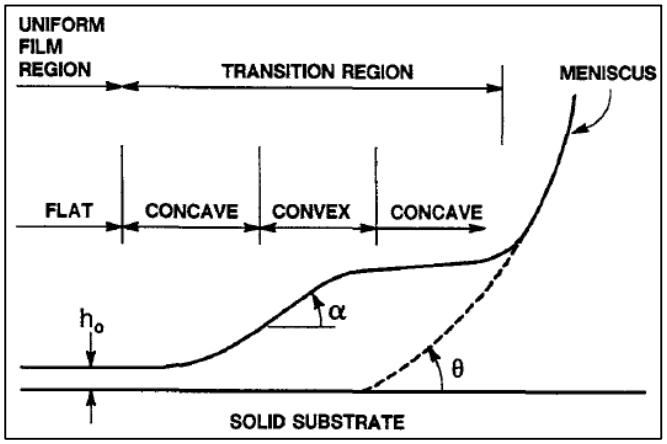

Figure 2-7: Profile of film/meniscus transition zone (Hirasaki, 1991)

2.2.3.3 Disjoining Pressure Components

The disjoining pressure is dependent on the intermolecular or interionic forces, and is composed of contributions from van der Waals, electrostatic, and solvation forces. DLVO theory relates these forces to give the disjoining pressure.

van der Waals Interactions. These are the sum of Keesom, Debye and London dispersion forces. They are represented by the Hamaker constant which can be calculated by various models, using the refractive index, dielectric constant, and absorption frequencies of the materials - all dependent on brine composition. They are attractive forces that work to bring two interfaces (oil/brine and brine/rock) together.

Electrostatic Interactions. These forces arise from a change in the system energy as two charged surfaces approach (electrical double layer interaction). These forces are the electrical contribution to the disjoining pressure. Models for calculation depend on several parameters including the Debye length, which is in turn dependent on electrolyte valence and concentration. This dimensional distance over which the interactions become important is approximately inversely proportional to the square root of concentration: as

the electrolyte becomes more concentrated, the distance over which two charged surfaces interact, decreases.

Solvation forces. Solvation forces are based on solvent molecule interactions with other ions e.g. hydrogen-bonds with other water molecules or specific ion/water interactions. These are also dependent on the pH and electrolyte composition; as the solute concentration increases, the repulsive forces between oil/brine and brine/mineral interfaces is said to tincrease.

Figure 2-8 shows an example set of disjoining pressure isotherms. For electrolyte concentrations above 1.0M, the isotherm is dominated by the van der Waals forces except at small thicknesses, where the structural forces are important. The formation brines in this study are approximately 4-6M, so the film thickness is expected to be very thin.

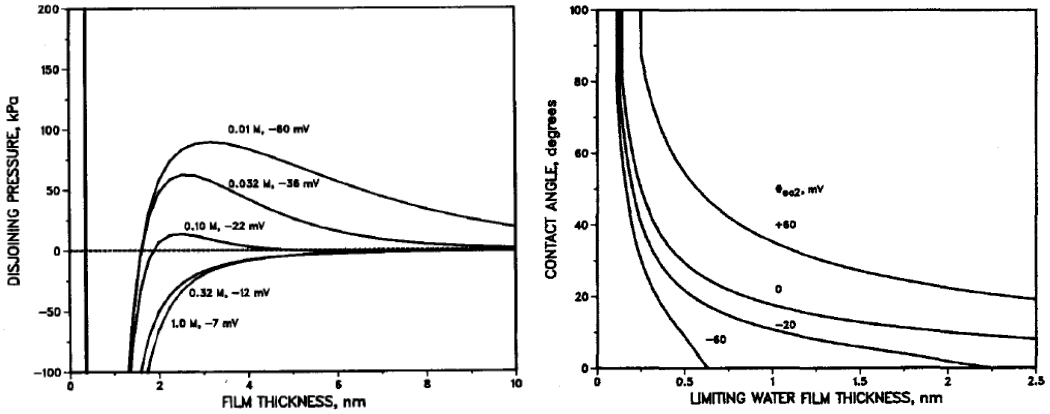

Figure 2-8: A) Example disjoining pressure isotherms for different electrolyte concentrations and set ion density and Hamaker constant; B) θ as a function of the post-draining, stable film thickness (concentration=0.1M) (Hirasaki, 1991)

2.2.3.4 Effect of Surface Forces on Contact Angles

The van der Waals forces are attractive, the electrostatic forces are generally repulsive, and the solvation forces are repulsive and dominant when the film is very thin. The van der Waals forces cause the brine film to drain until solvation forces come into

play and limit the film thickness reduction. If solvation forces were absent the film would drain to zero thickness and contact angles would be oil-wet, i.e., >90^o. As the equilibrium film thickness resulting from solvation forces increases, the contact angle decreases. If a dehydrated mineral surface is first contacted with oil, a large contact angle can result when it is subsequently contacted with water. Conversely, if the mineral has a layer of hydration only a single layer thick, the contact angle will be <90^o.

Initially reservoir rocks are completely filled with brine; oil invades the formation where the receding water contact angles control the interface movements. This movement may leave a hydration layer between the oil and the mineral. After equilibrium over geologic time, water flood in such a system may give a complex fluid arrangement as indicated in Figure 2-9.

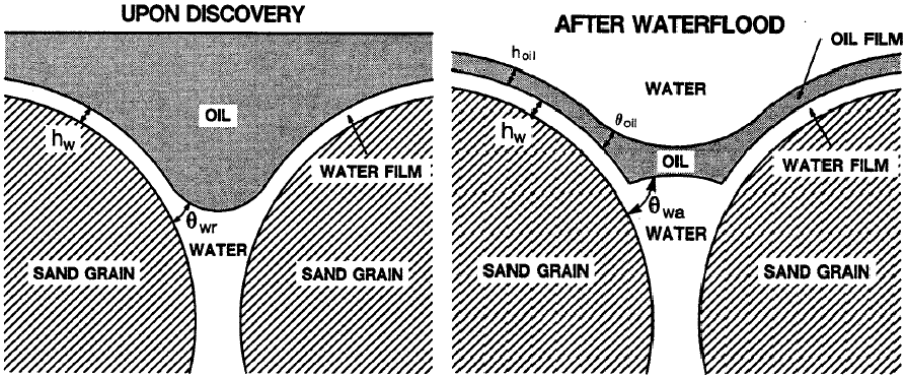

Figure 2-9: Thin films and contact angles in rock pore space (Hirasaki, 1991)

2.2.4 Wetting by Crude Oil

Prior to use in experiments, cores are restored to their natural state by aging in crude oil under high temperature. Electrical interaction of polar groups and ions in the COBR (core-oil-brine) system determines the equilibrium wetting state.

2.2.4.1 Electrical Double Layer

Carbonates have a point of zero charge around pH 9, below which the rock wall carries a positive charge. This charge induces the neighboring electrolyte to arrange itself such that ions of the opposite charge to the mineral surface are in closest proximity to the surface. These ions do not touch the surface due to slight motion from thermal fluctuations, but they remain in a thin layer surrounding the mineral surface with increasing concentration as the distance to the surface decreases (Schechter, 1992). Figure 2-10 shows a sketch of the double layer. The Stern layer is the immobile layer of counter-ions, while the diffuse layer changes thickness based on the bulk electrolyte composition, and the counter-ions outnumber their opposite.

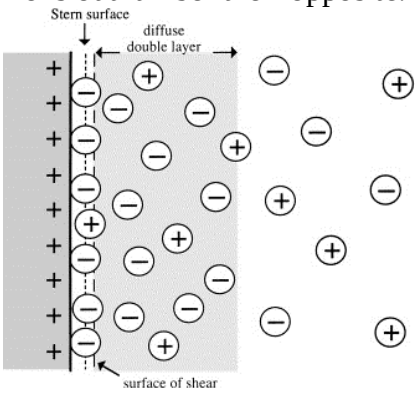

Figure 2-10: Sketch of electrical double layer indicating surface charge density vs. distance

2.2.4.2 Crude Oil Wetting

It is assumed that petroleum reservoir rock was initially saturated with brine and later invaded with crude oil. Thus, in the initial state there is a film of water between the rock and the oil. The rock type, brine composition, oil composition and pressure/temperature conditions all determine what the equilibrium wetting state will be over geologic time, i.e., if the crude oil can thin and break through the water film (Morrow, 1990). Reservoir conditions are typically conducive to this wettability change,

and oil composition is believed to be the next most important factor. The wettability altering components in crude oil are believed to be molecules consisting of a hydrocarbon and a polar or charged end. The polar/charged end can adsorb on the rock surface, exposing the hydrocarbon end free to interact with the bulk oil phase and exhibiting the oil-wet state. The diverse nature of these active agents makes their study difficult.

The crude oil's active components are distributed in the oil but prevalently found in the heavier fractions of resins and asphaltenes. These compounds contain oxygen, nitrogen and/or sulfur functional groups whose polar properties aid interaction with brine and rock surface (-OH, $-SO_3^-$, $-NH_2$, and $-COO^-$ to name a few). The oxygenated compounds are usually acidic and include phenols and various carboxylic acids. Results from Morrow (1990) verify that thinning and rupture of the water films are prevalent in carbonates since the mineral/brine interface is oppositely charged from the negatively charged brine/oil interface. For lower electrolyte concentrations, the electrostatic force is positive and significant. Thus the brine film stabilizes at a thicker value, and gives water-wet contact angles. It is difficult to make the rock oil-wet when aging with a low electrolyte brine.

The total acid number (TAN) is based on an acid-base titration that can give an idea of the quantity of active acid groups in a particular oil (ASTM D974). The validity of TAN sufficiently representing oil activity is debatable. The wettability-altering ability of these compounds has been extensively studied, watching water-wet mineral surfaces turn oil-wet. The highest acid number published in low salinity studies is 2.07 mg KOH/g oil (Zhang et al., 2007). Buckley (1998) summarized the mechanisms of oil adsorption to the rock surface (Figure 2-11) which include a) oil component polar interactions, b) asphaltene precipitation from oil- incompatible solvent mixtures, c) acid/base interactions, and d) ion binding assisted by multivalent ion.

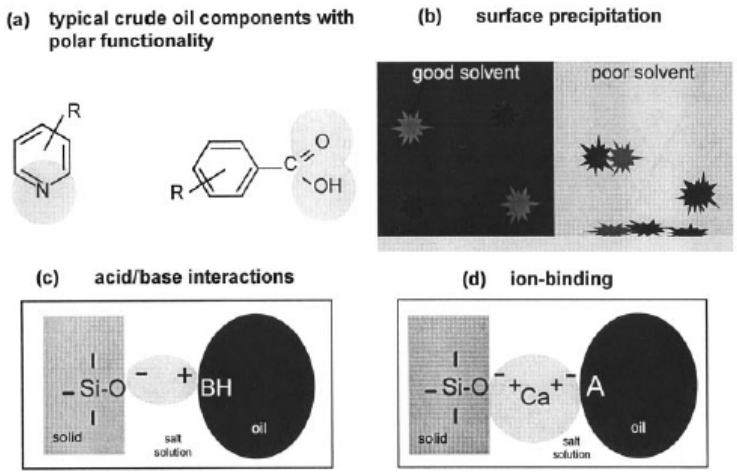

Figure 2-11: Mechanisms of Interaction between crude oil components and solid surfaces

2.2.5 Spontaneous Imbibition

2.2.5.1 Introduction and Ideas

One step in the Amott test process is the static spontaneous imbibition using the fact that the wetting fluid will imbibe into a core and non-wetting fluid will be expelled. Oil-aged cores are placed in imbibition cells filled with a bulk test fluid, and the oil recovery is noted as a function of time, typically one month. The experiment can be conducted at reservoir temperatures, but around atmospheric pressure. The process is governed by a balance of capillary and gravity forces. The potential of a wettability altering agent can be evaluated since expelling oil would require the test fluid to enter the core by imbibition, only possible if it can become the wetting fluid. The rate of recovery and final core saturation helps to compare test formulations.

The static imbibition experiment models the fracture-matrix interaction or the flow from a high permeability zone to an adjacent low permeability zone. The dynamic imbibition experiment is a better model; the test formulation is injected through an induced/artificial fracture in a core and any oil recovery is directly related to the extent of

imbibition. The batch experiment is much simpler to perform, thus preferred and discussed here.

Spontaneous imbibition can see two types of recovery: a) co-current imbibition occurs when both the inlet and outlet of a core are open to a test fluid; the displacing and displaced fluids flow in the same direction, and b) counter-current imbibition where only one core end is open; the invading fluid enters through this opening, and the displaced fluid flows in the opposite direction, out through the same opening. Formulations containing surfactants giving ultra-low IFT mitigate the capillary pressures in the system, giving oil recovery mainly from the top of the core i.e. co-current imbibition where the test fluid enters from the sides and bottom and oil exits from the top. Brine formulations with high water-oil IFT give counter-current imbibition: the port of entry of invading fluid is the port of oil exit.

2.2.5.2 Scaling of Spontaneous Imbibition

Spontaneous imbibition rates and final recoveries are affected by rock, oil and brine properties, thus scaling of experimental recovery versus time data has been thoroughly investigated, aiming to collapse data from similar COBR systems into a single curve. Mattax and Kyte (1962) proposed a scaling model for the case with dominant capillary forces:

$$t_d = Ct\sqrt{\frac{k}{\varphi}}\frac{\sigma}{\mu_w}\frac{1}{L_c^{\,2}} \qquad (2\text{-}6)$$

where t_d=dimensionless time, C=unit conversion factor, t=absolute imbibition time, k=permeability, φ=porosity, σ=IFT, μ_w=invading fluid viscosity, and L_c=characteristic length of core. The model assumes that samples of interest a) are of the same shape and orientation, b) have the same oil/water viscosity ratio, c) have similar initial fluid saturation/distribution, d) have similar relative permeabilities, and e) have similar

capillary pressure curves. Assumptions c, d and e imply that the rock pore structures are the same. The model also specifically applies to water-wet rock.

An adjustment to equation (2-6) was made by Ma et al. (1999) better accounting for the rock dimensions and including oil viscosity. The main equation remains the same but μ_w is replaced by $(\mu_w . \mu_o)^{½}$, and $L_c=0.5(Ld)/(d^2+2L^2)^{½}$, where d is the core diameter. The modification gave a much better fit with the very strongly wet core imbibition data.

Many more adjustments and models have been developed to account for other parameters e.g. gravity forces (Xie and Morrow, 2001) or oil-wet rock surfaces. The characteristic that has proven difficult to model is the fact that wettability is in the process of changing when wettability altering agents are tested by imbibition i.e. that the wettability is not fixed during the process.

The dominant forces can be quickly deduced from the dimensionless Bond number that gives the ratio of capillary forces to gravity forces (Schecter et al., 1994):

$$N_B^{-1} = C\frac{\sqrt{\frac{\phi}{k}}\sigma}{\Delta\rho g L} \qquad (2\text{-}7)$$

where C=dimensionless constant (0.4), Δρ=density difference of fluids.

2.2.6 Wettability Effects on Waterflooding

Waterflooding efficiency is strongly affected by rock wettability as seen from 1D core displacement experiments, and is the base case against which EOR methods are compared. The fluid distribution in different wetting states was described previously and helps to explain trends seen (Figures 2-3 and 2-9). The flow behavior can be captured by the relative permeability (during the two phase flow of oil and water, each phase travels at a different rate and depends on core saturations) shown in Figure 2-12A. Dependence of oil recovery on the rock wettability is shown in Figure 2-12B. The figure shows very

strongly water-wet or preferentially oil-wet systems to give the lowest recovery (Amott-Harvey (A-H) indices closest to 1 and -0.5 respectively), while the optimum recovery is at slightly water-wet A-H index of 0.1 to 0.3 (Morrow, 1990).

For a fully water-wet core at high initial oil saturation, water occupies small spaces and oil remains in larger pores, both phases being connected and continuous. At the start of waterflooding the oil relative permeability (k_{ro}) is high, since oil flows through the largest pores, but decreases as the saturation decreases. The water relative permeability (k_{rw}) is initially low but increases as water saturation increases. The water occupies increasingly larger pores, sometimes surrounding an oil filled pore that has not drained, thus trapping the oil (target oil of EOR). Water continues to fill all flow paths and the oil stops flowing i.e. the end point relative permeability (k^o_{rw}) is reached. For reasonable mobility or viscosity ratios, most of the recoverable oil is produced prior to water breakthrough.

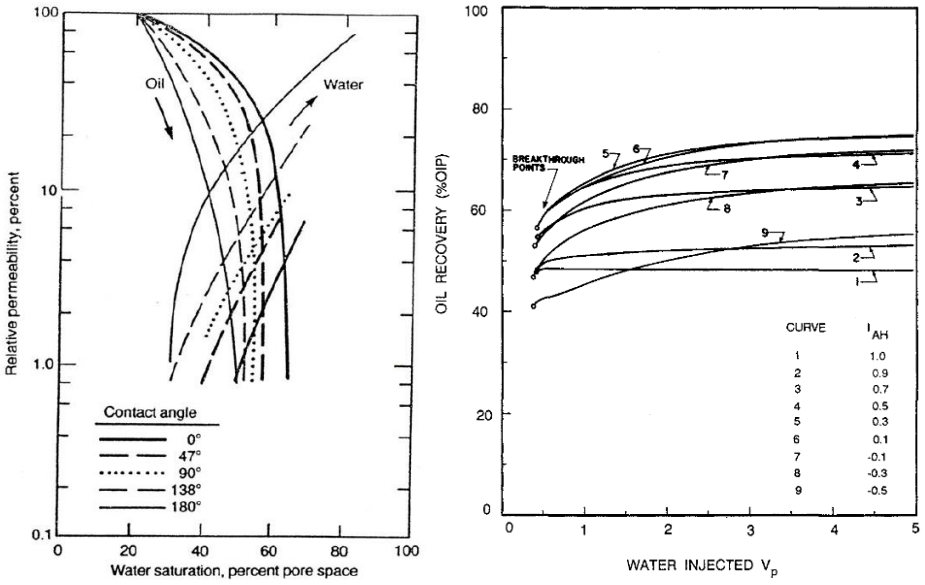

Figure 2-12: A) Relative permeabilities for range of wetting conditions; B) Oil recovery from cores at different wettability indicated by the Amott-Harvey index (Morrow, 1990).

When waterflooding a mixed or oil-wet core, the water relative permeability is higher than the water-wet case, and the oil relative permeability is lower. The water flows more easily because it travels through pore centers, the higher velocity causing earlier breakthrough. However, water does not penetrate smaller pore spaces occupied by the oil thus giving poorer recovery at breakthrough, due to poorer sweep. In this case, oil is produced for many pore volumes (PV) of water injected, and high residual oil saturation (S_{or}) remains.

Figure 2-12B shows the ultimate oil recovery varying up to 35% original oil in place (OOIP) depending on the wettability. Altering the wettability during a waterflood would thus be a beneficial process to study, ensuring water to enter the smallest pores containing oil, and reduce the S_{or}. An overview of the mechanisms of wettability alteration is given next.

2.3 MECHANISMS OF WETTABILITY ALTERATION

2.3.1 Low Salinity Brine Effects in Sandstones

The response of sandstone permeability to low salinity water flooding was investigated by Baptist & Sweeney (1954) who showed that the amount and type of clay content was important. The effect of brine composition on water flood oil recovery has been studied by Morrow and coworkers [Jadhunandan, 1990; Jadhunandan & Morrow, 1995; Yildiz & Morrow, 1996; Tang & Morrow, 1997] who showed improved oil recoveries in Berea sandstones when flooded with a low salinity brine.

Five possible mechanisms are proposed to contribute to the increased oil recovery in sandstones during low salinity water floods:

1. Fines migration, where fines detach from pore walls under certain brine salinity and composition, polar components of oil attached to fines also detach along with

fines improving water-wetness and oil recovery (Tang & Morrow, 1999; Tang & Morrow, 2002; Doust et al., 2009);

2. Increase in pH, which may lead to in-situ soap generation lowering the interfacial tension and the residual oil saturation (Webb et al., 2004; McGuire et al., 2005);
3. Multi-ion exchange, where divalent cations adsorbed on the solid surface are exchanged with monovalent cations, polar oil molecules attached to the divalent cations are also released leading to increased water-wetness (Lager et al., 2006; Lager et al., 2007);
4. Mineral dissolution, specifically mixed-wet calcite cement with attached oil polar groups may detach from pore walls releasing oil (Pu et al., 2008);
5. Double layer effects: decreasing brine salinity and multivalent ion concentrations cause the electrical diffuse double layer between clay and oil particles to expand, in turn giving increased electrostatic repulsion which may cross the threshold binding force between clay and oil, releasing the oil from the rock surface and changing the rock wettability (Ligthelm et al., 2009; Lee et al., 2010).

These findings have led to further studies, such as, field tests, evaluation in secondary versus tertiary recovery mode, and combination of low salinity with surfactants and polymers (Kozaki, 2012).

2.3.2 Low Salinity Brine Effects in Carbonates

2.3.2.1 Multi Ion Exchange

Analogous research on carbonates is less comprehensive, but similar mechanisms have been proposed for changing rock wettability from oil-wet to water-wet, and subsequently oil recovery, by brine composition manipulation. Austad and coworkers have made significant progress in the study of high temperature chalk systems (Austad et.

al, 2005; Hognesen et al., 2005; Strand et. al, 2006; Zhang & Austad, 2005; Zhang et al., 2007, Austad et al., 2008) conducting systematic spontaneous imbibition tests for varying crude oil acid number, temperature, and brine ion concentrations. A multi-ion exchange mechanism that explained many of the Austad group's findings was proposed in Zhang et al. (2007) [Figure 2-13]. The divalent ions, Ca^{2+}, Mg^{2+} and SO_4^{2-}, naturally present in seawater, were deemed to be potential determining ions based on zeta potential measurements. The mechanism follows the following reaction:

$$RCOO^- - CaCO_{3(s)} + Ca^{2+} + SO_4^{2-} = CaCO_{3(s)} + RCOOCa^+ + SO_4^{2-} \quad (2\text{-}8)$$

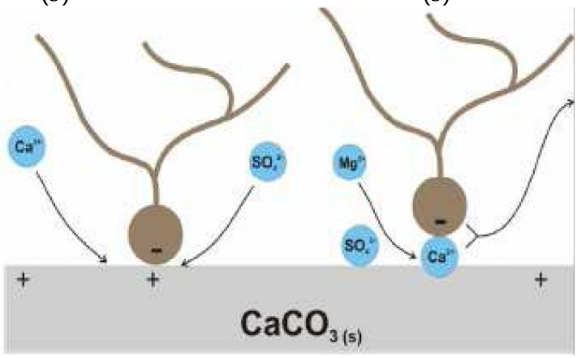

Figure 2-13: Proposed multi ion exchange mechanism (Zhang et al., 2007)

The divalent anion (SO_4^{2-}) is said to compete with the acid group of the crude oil molecule to attach to the surface of the chalk, following which the divalent cations compete to attach to the rock surface to mitigate charge imbalance, leading to the acid group detaching from the carbonate surface and changing the wettability. The anion requires the presence of a divalent cation to promote this mechanism and vice versa i.e. a symbiotic relation. High temperatures speed up the mechanism, and specifically increase the activity of the Mg^{2+} ion (Strand et al., 2006; Puntervold et al., 2008) to pair with the rock surface carbonate anions. With successful results in chalk, the work was extended to limestone reservoir rock (Strand et al., 2008) which has a significantly smaller specific

surface area, however similar response to brine composition and temperature variation was observed. Doust et al. (2009) suggested that the multi ion exchange could also take place at high invading brine salinity as long as the relative divalent cation contents differed between the invading and connate brines.

2.3.2.2 Dissolution

Dissolution of carbonates has been well document in geology and groundwater research. Injection of a brine not in equilibrium with the carbonate can push mineral-brine kinetics towards dissolution which can lead to wettability alteration as a fresh rock layer, untouched by oil, is exposed. Observations at high temperatures and pressures are abundant.

Hiorth et al. (2008) developed a thermodynamic model based on aqueous chemistry, surface adsorption, and mineral dissolution/precipitation to calculate the surface charge behavior of the rock in response to different brine properties. They modeled the Austad group's work in chalk and concluded that surface charge changes did not correlate with the oil recovery, but instead suggested a dissolution mechanism that explained the increase in recovery with temperature. At lower temperatures, calcite is in equilibrium with seawater, but at higher temperatures calcium in the seawater reacts with sulfate and precipitates anhydrite. The aqueous phase loses calcium, but to maintain the equilibrium with the rock surface, calcium dissolves off the solid surface into the brine. Adsorbed oil may also be released from the surface with the calcium, thus leading to enhanced imbibition oil recovery.

Proponents of the multi ion exchange mechanism have debated the validity of dissolution playing a role in the chalk spontaneous imbibition experiments. Austad et al. (2009) present results where high Ca^{2+} concentrations in the presence of SO_4^{2-} improved

imbibition oil recovery instead of inhibiting carbonate dissolution. A counter theory involving dissolution involves the presence of anhydrite in the core that converts to gypsum in the right conditions (Austad et al., 2012), anhydrite detach off the surface and attached oil molecules leave with it.

Yousef et al. (2010) have conducted low salinity core floods in limestone cores and found incremental tertiary recovery with sequential dilution of seawater up to 18% OOIP beyond the sea water flood. Continued study including contact angle experiments (Figure 2-14) led them to conclude that wettability alteration occurred and microscopic dissolution was a contributing mechanism (Yousef et al., 2012a). They conducted a single well test (Yousef et al., 2012b) with low salinity brine which yielded a reduction of residual oil saturation by 7%.

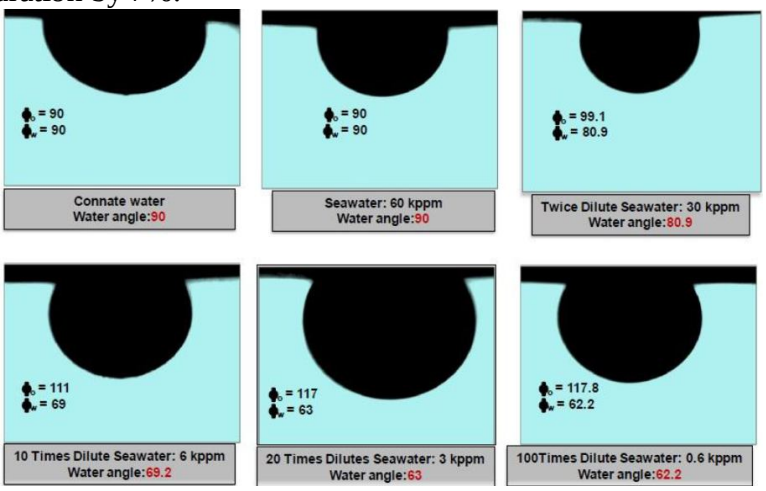

Figure 2-14: Contact angle study showing increased water-wetness for decreasing brine salinity (Yousef et al., 2010).

Zareteskiy (2012) built a 1D flow model (incorporates aqueous chemistry, surface adsorption, and mineral dissolution & precipitation) to capture low salinity effects in chalk. He concluded the occurrence of both multi ion exchange and mineral dissolution and that the injection flow rate & temperature dictate which mechanism was faster and

dominant. Romanauka et al. (2012) used spontaneous imbibition to show that lowering ionic strength gave incremental oil recovery probably due to wettability alteration, but dissolution could not be confirmed. Zhang & Sarma (2012) found low salinity to be more effective than increasing sulfate content at a low temperature, but equally effective at a high temperature. They also found *fines migration* to play a key role in improving "smart-water" flooding performance.

2.3.2.3 Alternative Oxidizing Agents

The sulfate anion's importance in altering wettability has been well documented by the Austad group. It is a good oxidizing agent (the sulfur exists at a high oxidation state leading to high electronegativity), and it has a high charge density (the estimated ion radius is 1.49Å). Gupta et al. (2011) and Vo et al. (2012) investigated alternative potential determining ions such as borate and phosphate: contact angle experiments showed favorable wettability altering behavior, however calcium and magnesium salt precipitation also occurred. The authors showed that the supernatant from a centrifuged sample was suitable for core flooding and wettability alteration testing, but the practicality of this process is questionable. Incremental oil recoveries were obtained when a core was flooded with seawater with added sulfate, phosphate or borate.

Chen (2012) studied the addition of EDTA to surfactant solutions for use in fractured dolomite rock. EDTA with and without surfactant caused dolomite dissolution at 100C. Alternative oxidizing agents should be researched for greater control over the rates of wettability alteration.

Chapter 3: Materials and Experimental Procedures

This chapter describes the method, materials and experimental procedures used to identify wettability altering low salinity brines for the given COBR system. A screening process is used to narrow down candidate brines with calcite plate contact angle tests being the first filter. Successful brines are confirmed for wettability altering ability in spontaneous imbibition tests then core floods.

3.1 MATERIALS

3.1.1 Crude Oil

Oils from two carbonate reservoirs (A & B) are used in this work. Both oils are fairly light: at room temperature oil A has a density of 0.86g/cm^3 and oil B has a density of 0.82 g/cm^3 at 25^{o}C (reported as API 40). The viscosity behavior with temperature is shown in Figure 3-1: oil A is 5.3 cp at room temperature and about 1.4 cp at the reservoir temperature of 120^{o}C. Oil B is 3.4 cp at room temperature and decreases to 1 cp at reservoir temperature. The Andrade equation,

$$\ln(\mu) = \ln(A) + B/T \qquad (3\text{-}1)$$

characterizes oil viscosity versus temperature behavior accurately. The oils were always filtered through 0.5 μm filter to remove any particulates with potential for core plugging.

Further properties of Oil A are not available, but Oil B analysis results are listed. The total acid number (TAN) is determined by repeated titrations with KOH and Phenolphthalein color indicator. The measured TAN for oil B is 2.45 mg KOH/g oil.

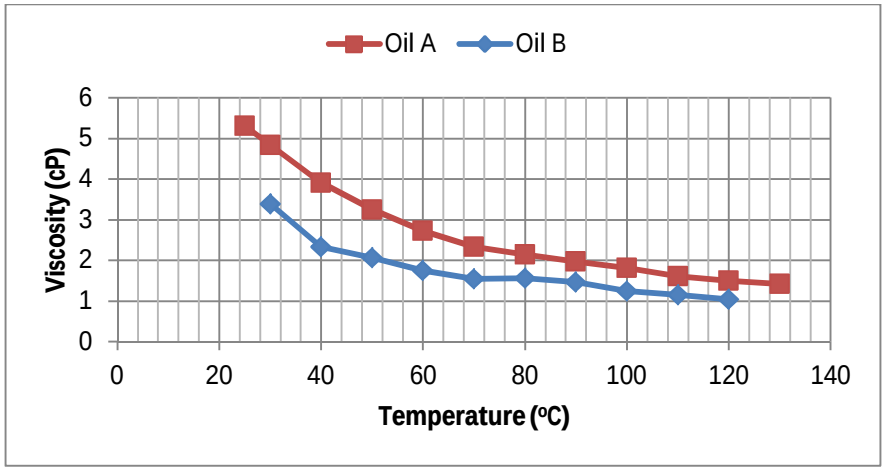

Figure 3-1: Viscosity versus temperature behavior of reservoir oils at shear rate $1s^{-1}$

SARA analysis (Figure 3-2) shows a notable asphaltene content around 0.25 wt%. The initial reservoir pressure was reported at 4180 psig, with bottom-hole production pressure at 3700 psi.

Summary of Stock Tank Oil Analysis

Analysis	Results	Method
Wax Content, wt %	4.11	UOP 46
Sulphur, wt %	0.82	ASTM D-129
Wax Appearance Temperature, °F	84.0	CPM
Asphaltene content (unfiltered), wt %	0.28	IP 143
Asphaltene content (filtered), wt %	0.23	IP 143

SARA Analysis by Iatroscan

Analysis	Results
Hydrocarbons/Non-Hydrocarbons Ratio, wt/wt	10.4
Saturates Fraction, wt %	44.9
Aromatics Fraction, wt %	46.3
Saturates/Aromatics Ratio, wt %	1.0
Resins (NSOs) Fraction, wt %	6.7
Asphaltenes Fraction, wt %	2.1
Resins/Asphaltenes Ratio, wt/wt	3.2

Figure 3-2: SARA analysis of oil B

3.1.2 Brine

The brines were synthesized using deionized water and the four main salts of NaCl, $MgCl_2.6H_2O$, $CaCl_2.2H_2O$, and Na_2SO_4, all at least at 99.3% purity from Fisher Chemicals. The formation brine (FB) for this reservoir is very saline at 179,700 ppm. The composition for the formation brines for the two reservoirs are detailed in Table 3-1. Other important brines used in this study are listed in table 3-2. The seawater is named SW. Seawater diluted with deionized water in the proportion of 1:20 is named SW/20, and fifty times diluted seawater is termed SW/50.

Ions (ppm)	FB-A	FB-B
Na+	56200	49933
Mg2+	19800	3248
Ca2+	770	14501
Cl-	56	111810
SO42-	96	234
HCO3-	124100	-
Ionic Strength	4.642	3.658
TDS (mg/L)	201,022	179,730

Table 3-1: Formation brine compositions for reservoir A and B

Ions (ppm)	SW	Mg Ca 4S	0Mg 0Ca 4S	Mg 0Ca 0S	SW/20	SW/50
Na+	13700	11398	16967	15547	685	274
Mg2+	1620	1620	-	1620	81	32.4
Ca2+	521	521	-	-	26.05	10.42
Cl-	24468	13452	16392	28702	1223.4	489.36
SO42-	3310	13240	13240	-	165.5	66.2
Ionic Strength	0.871	0.873	0.876	0.876	0.044	0.017
TDS (mg/L)	43,619	40,230	46,599	45,869	2,181	872

Table 3-2: Composition of important brines used in study

Modified brine compositions are based on SW composition and the naming convention reflects the relative change in the concentration of the divalent ions of

interest. The Ca^{2+} concentration of the modified brine xCayMgzS is x times the Ca^{2+} concentration in SW. Similarly, Mg^{2+} concentration is multiplied by a factor of y, and SO_4^{2-} concentration is multiplied by a factor of z. The brine MgCa4S indicates seawater composition with quadrupled SO_4^{2-}concentration. Modified brine compositions were adjusted from seawater composition by maintaining the ionic strength rather than the total dissolved solids.

3.1.3 Reservoir Rock

Reservoir cores of 1.5 inch diameter and varying length were used. Table 3-3 shows the core properties for reservoirs A and B. Reservoir A rock is tighter than reservoir B rock. As expected of carbonate reservoirs, the properties vary over a large range indicating the field heterogeneity; the order of magnitude indicates low permeability rock. Cores are reported to be composed of primarily limestone with little dolomite. Figure 3-3A is representative of the cores, and shows some crystal growth on the surface.

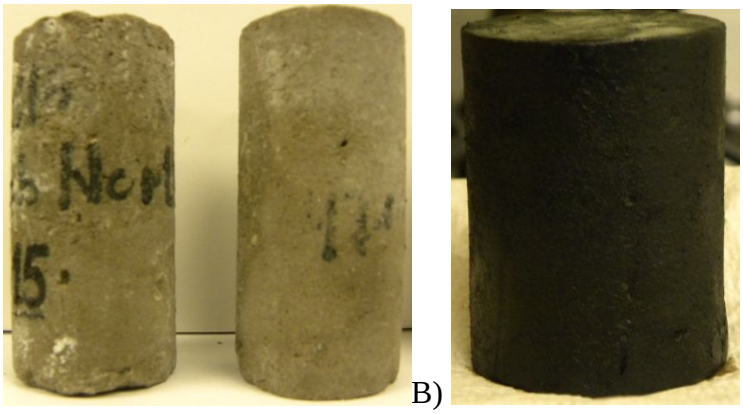
B)

Figure 3-3: Example reservoir cores used in experiments A) initial state, B) aged state

	Flood	Diam (mm)	Length (mm)	PV (cm^3)	Porosity	S_{oi}	k_{air}	k_{brine}	$k_o@S_{wirr}$
A	CF A1	38.4	91.9	17.9	13.9	0.8	6.1	4.4	-
B	CF B1	37.7	74.4	15.3	19.1	0.68	63.4	40.9	17.7
	CF B2	37.4	78.0	14.6	17.8	0.79	70.4	23.2	2.9
	CF B3	37.9	55.9	16.7	26.4	0.68	38.4	7.6	6.2
	CF B4	37.9	52.9	15.8	26.4	0.68	38.4	7.6	1.5
	CF B5	37.7	75.9	13.3	15.5	0.76	64.7	10.3	
	CF B6	37.7	72.0	12.3	15.5	0.76	64.7	10.3	
	CF B7	37.9	74.0	11.4	12.9	0.84	13.4	16.8	
	CF B8	37.9	74.0	11.4	12.9	0.84	13.4	16.8	
	Imb B9	37.4	78.2	21.8	25.3	0.56	76.6	22.6	-
	Imb B10	37.4	78	21.9	25.6	0.77	70.4	9.5	-
	Imb B11	37.7	72.6	15.4	18.9	0.74	39.6	11	-
	Imb B12	37.9	75	12.2	14.4	0.53	72.5	5.1	-

Table 3-3: List of cores and associated properties

3.2 PROCEDURES

3.2.1 Core Preparation & Characterization

Reservoir cores were restored with dead reservoir oil and aged prior to use; the pore volume and permeability to air was measured followed by CO_2 flooding and vacuuming prior to brine saturation and characterization. The brine filled core was then flooded with oil with a very high pressure drop to bring the core to the connate water saturation or initial oil saturation. The core was then aged in the reservoir oil at 80^oC for at least 30 days.

Cores were recycled for use in subsequent experiments and were cleaned accordingly. Dean-Stark extraction used a 65% chloroform and 35% methanol solvent mixture at 65-80^oC that was refreshed until only traces oil was recovered. This process cleaned the core sufficiently. As cleaning is suspected to affect ion concentrations at the

rock surface, many pore volumes of the formation brine were run through the core before oil saturation.

3.2.1.1 Porosity

Porosity is the fraction of void volume over the bulk volume. The Boyle's law based gas expansion porosimeter was employed (Figure 3-4). The method is non-destructive and provides a reasonable first estimate of the pore volume, prior to accurate measurement with brine.

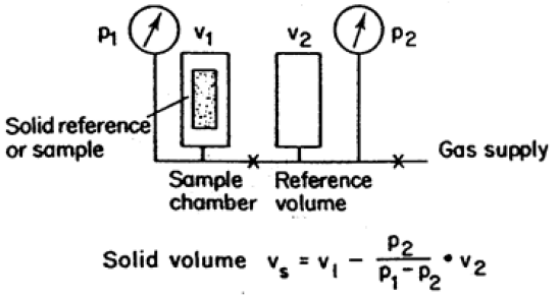

Figure 3-4: Sketch of porosimeter based on Boyle's Law

3.2.1.2 Permeability

The absolute permeability is defined in Darcy's law and used to characterize the single phase fluid flow in a core.

Single phase, incompressible (brine): $$q = \frac{kA}{\mu}\frac{\Delta P}{L} \quad (3\text{-}2)$$

Single phase, compressible (gas): $$q_{sc} = \frac{kA}{2\mu P_{sc}}\left(\frac{P_1^2 - P_2^2}{L}\right) \quad (3\text{-}3)$$

where q is the fluid flow rate at the reference pressure, k is the permeability to the testing fluid, A is the cross sectional area of the core, μ is the fluid viscosity, $\Delta P = P_1 - P_2$= the difference between pressures at the inlet and outlet respectively, L is the core length, and P_{sc} is the reference pressure.

3.2.2 Contact Angle

Calcite mineral blocks are broken into flat 0.5” x 1” x 0.25” plates and polished using a diamond grinder for a smooth and uncontaminated surface. The polished plates are first aged in the formation brine for 3 days at 80^{o}C, followed by aging in the reservoir oil for 20 days at a temperature of 80^{o}C to render them oil-wet (same procedure as that used for cores, smaller time frame). To ensure the plates are oil-wet, a formation brine drop is placed on the aged plate and the contact angle is observed; if the drop gives an oil-wet contact angle then the plate is submerged in formation brine for 1-2 hours to note that oil still sticks to the plate. At this point the calcite plate is submerged in the test brine. The oil-wet plate submerged in test brine is placed in the oven at the test temperature (90-100^{o}C). Photographs are taken to document the time-variant behavior. When the drop reaches an equilibrium angle, the contact angle is assessed with a goniometer.

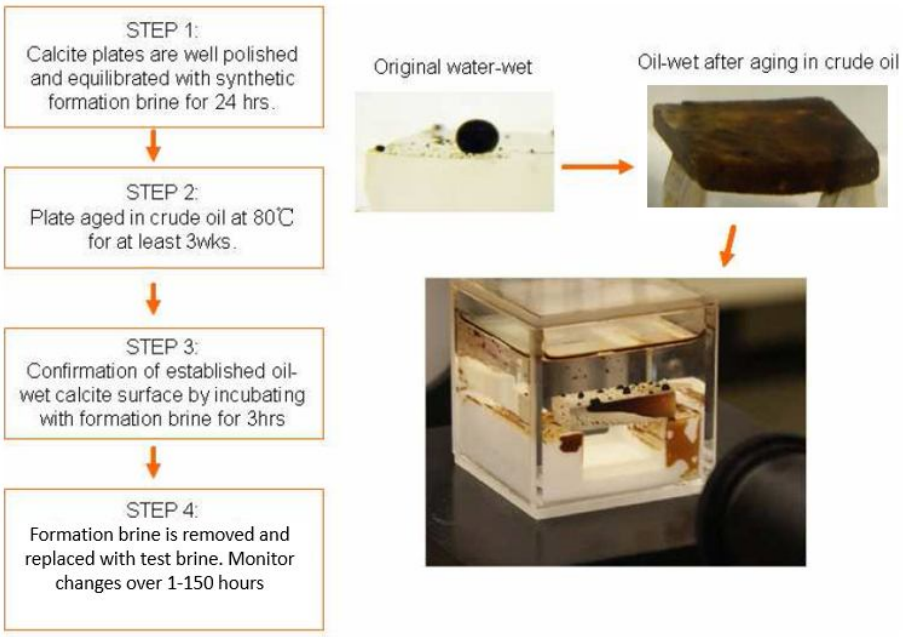

Figure 3-5: Steps and typical view of contact measurement on calcite surface (Chen, 2012 adjusted)

Figure 3-5 summarizes the steps and indicates the evolution of a calcite plate's wettability that is also expected with aged cores due to low salinity brine. The measured angles are water-advancing contact angles, i.e., the water encroaches in a space previously occupied by oil. This is the angle that is relevant to the waterflooding of the reservoir.

3.2.3 Spontaneous Imbibition

Clear, glass cells house core plugs for imbibition experiments (Chen, 2012). The cell is capped such that pressures higher than 1 atm can be maintained at elevated temperatures. Prior to use, aged cores are confirmed to be oil-wet by first immersing in formation brine at room temperature and raising the temperature in increments to the reservoir temperature (120°C). The temperature is first raised to 60°C and allowed to equilibrate for 1 hour, then raised to 80°C and allowed to equilibrate for another 1 hour, and this process is repeated in 10°C increments with equilibration at each temperature. Even if the core is oil-wet, the temperature rise causes some thermal expansion of the core's fluid contents; thus some oil is recovered and the volume is recorded. The core is monitored for several hours at the reservoir temperature to check that the recovered oil volume does not change appreciably post thermal expansion. If the volume remains constant then the core is deemed oil-wet and ready for wettability alteration experiments. The cell is removed from the oven and allowed to cool to room temperature. The formation brine in the cell is replaced with the test brine, recapped and again heated to reservoir temperature, recording any changes in oil volume through the heating process. The cell remains in the oven for at least 3 weeks and the recovered oil volume is recorded.

3.2.4 Core Flood

Hassler type core holders are used for core flooding at the reservoir temperature, and a back pressure of 50 psi is used to prevent boiling of water. The overburden pressure is set at about 650-700 psi. The interstitial velocity is set to 1 ft/day, which amounts to approximately 0.048 cc/min (depends on the specific core dimensions and porosity). 2 ml effluent samples are collected in a fraction collector to analyze the ionic composition of the effluent brine. The effluent pH is also monitored.

3.2.5 Effluent Analysis

The ion chromatograph instrument (Dionex ICS 3000) is used to analyze the ionic composition of the effluent. This precision of this instrument is in the range of 10ppm; it can only analyze samples of a maximum salinity of 4000ppm. The reservoir formation brine is approximately 50 times more concentrated than this upper limit; thus the effluent brine is diluted, based on the salinity level, prior to use in the ion chromatograph. The effluent samples from core floods are first separated from oil by filtering through a 0.22 micron filter then diluted for ion analysis.

Chapter 4: Results and Discussion

4.1 Aged Core Wettability

Rock from reservoirs A and B are very similar to each in composition. Core CF A2 was saturated and aged with oil and then used in the Amott process to determine the wettability after aging. The Amott-Harvey wettability index, I_{A-H} was determined to be -0.77. The brine imbibition step of an aged reservoir B core was conducted to confirm the oil-wetness in aged rock B: no brine imbibed and no oil was recovered at room temperature. Raising temperature to 80^{o}C recovered ~1 cm^3 of oil (less than 10% of the pore volume) within the first few hours; this was attributed to thermal expansion. Figure 3-3B shows the aged core and Figure 4-1 shows an oil drop on a reservoir B core inside an imbibition cell.

Figure 4-1: Reservoir B core in imbibition cell showing oil drop indicating oil-wetness

4.2 Contact Angle Experiments

A range of brines were synthesized by modifying the SW brine composition. The divalent ion content, Ca^{2+}, Mg^{2+} and SO_4^{2-}, was adjusted as previous studies have indicated that these are the potential determining ions or significant contributors to wettability (Zhang et al., 2007; Strand et al., 2008). The divalent ion concentrations were multiplied by factors of 0, 2 and 4; so the nine test brines (Table 4-1) were MgCa0S, MgCa2S, MgCa4S, 0Mg0Ca2S, 0Mg0Ca4S, Mg0Ca0S Mg0Ca4S, 0MgCa0S and

0MgCa4S. The chosen brines cover the combination, isolation and exclusion of the three divalent ions.

The experiments were conducted at 100^{o}C where mild boiling was seen and some oil left the calcite plate surface with gas bubbles that escaped solution. The drops that remain on the mineral surface vary in size, dependent on the location on the mineral surface. It is assumed that whether an oil drop remains on the mineral or leaves, is controlled by the balance between adhesive forces and buoyancy forces. Under oil-wet conditions the adhesive force will be strong and greater than an oil drop's buoyancy force. Under water-wet conditions, the adhesive forces are of the order of the buoyancy forces allowing only small drops to remain on the surface. Accordingly, areas of the calcite plate that are clear of oil or contain small droplets of oil are deemed water-wet, while other areas remain oil-wet. This lends to subjective and qualitative assessment of the wettability altering nature of a particular test solution, but as only the first filter in the screening process, it is acceptable. The mineral plate having water-wet and oil-wet sections demonstrates the wettability changing mechanism to be non-uniform.

4.2.1 Modified Brine

4.2.1.1 Reservoir B

Table 4-1 shows the compositions of brine tested; white cells in Table 4-1 indicate compositions that were not tested. Six of the modified brines tested gave promising results: MgCa2S, MgCa4S, 0Mg0Ca2S, 0Mg0Ca4S, Mg0Ca0S and Mg0Ca4S (shaded in green in Table 4-1). Figure 4-2 shows the results of tests with 0MgCa4S and is representative of the other successful contact angle tests. Unsuccessful compositions were 0MgCa0S, 0MgCa4S and MgCa0S (the plates simply continue to look oil-wet as in Figure 3-5), shaded in orange in Table 4-1.

		Magnesium Ion	
		0Mg	**Mg**
Sulfate Ion	**0S**	0Ca	0Ca
		Ca	Ca
	2S	0Ca	0Ca
		Ca	Ca
	4S	0Ca	0Ca
		Ca	Ca

Table 4-1: Grid showing combinations of modified brine tested in contact angle experiments at 100°C for rock B. Successful wettability alteration is shaded in green; unsuccessful formulations are shaded in orange. White background formulations were tested.

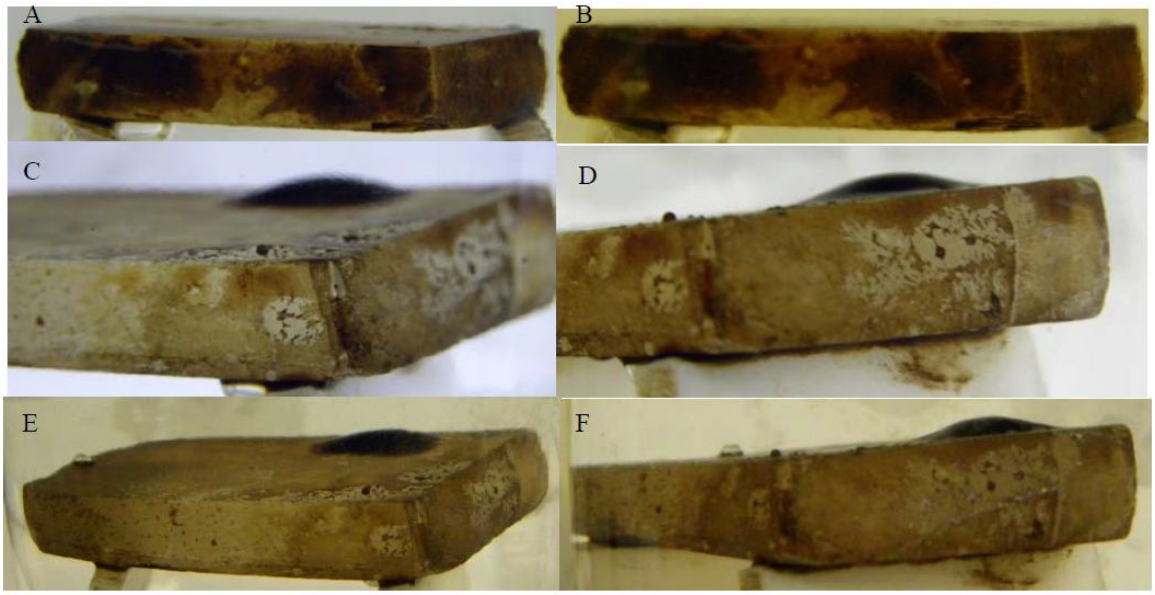

Figure 4-2: Calcite plate in 0Mg0Ca4S at 100°C initially (A, B); after 48 hours (C, D); after 5 days (E, F)

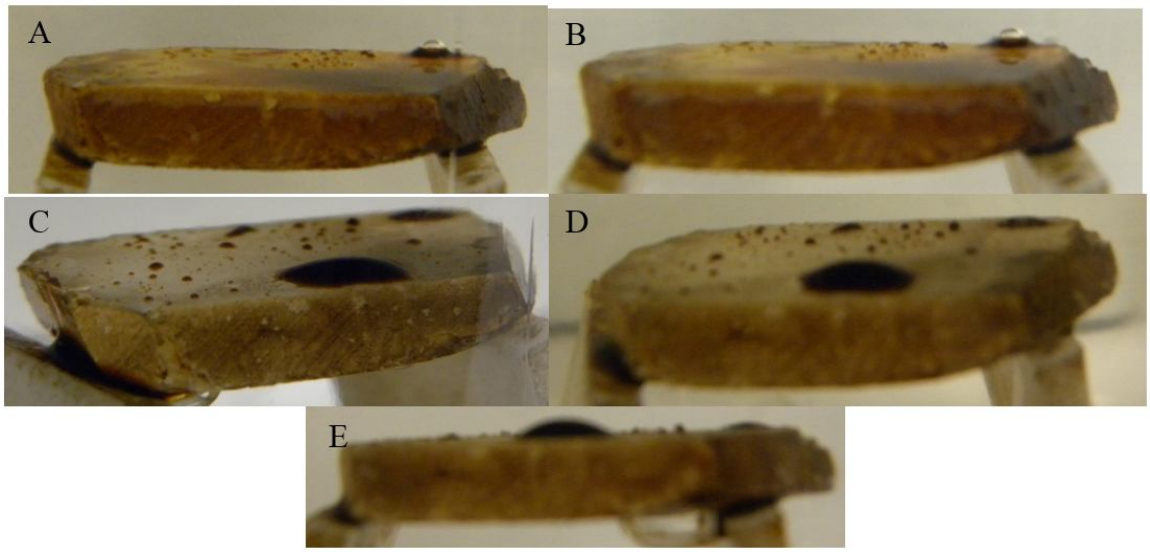

Figure 4-3: Calcite plate in MgCa4S at 100C initially (A, B); after 48 hours (C); after days (D, E)

The modified brines which gave large areas of mineral surface free of oil or containing very small oil drops, or a combination were deemed successful. The oil drops appeared to have at least intermediate-wet (75-115^{o}; Anderson, 1986) contact angles, if not water-wet angles (0-75^{o}). The unsuccessful formulations did not have any area of the mineral surface clear of oil. The results show that:

1. Brine with magnesium as the only divalent ion causes wettability alteration (Mg0Ca0S);
2. Brine with sulfate as the only divalent ion also causes wettability alteration (0Mg0Ca2S, 0Mg0Ca4S);
3. Magnesium and sulfate ions together, in the absence of calcium, cause wettability alteration (Mg0Ca4S);
4. Magnesium, sulfate and calcium ions altogether cause wettability alteration (MgCa2S, MgCa4S)

5. Calcium as the lone divalent ion (0MgCa0S), combined with sulfate (0MgCa4S), or combined with magnesium (MgCa0S) does not cause any wettability alteration.

This observation points to Mg^{2+} and SO_4^{2-} being the active potential determining ions for this rock and oil system, while Ca^{2+} presence in brine has a hindering effect when present in the concentration of SW brine. The inference is that Ca^{2+} coming off the mineral surface is a dominant mechanism in the wettability alteration, by Mg^{2+} substituting Ca^{2+} for a dolomitization effect shown to occur at high temperatures (Zhang et al., 2007; Strand et al., 2008). The effectiveness of sulfate as the lone divalent ion can be explained by the mechanism proposed by Zhang et al. (2007) specifically considering the competition with the oil's acid group. If these experiments were done on a plate made of calcite and anhydrite, then another mechanism that could occur is straight dissolution of the anhydrite (Austad et al., 2012).

4.2.2 Seawater Dilution

4.2.2.1 Reservoir B

Contact angle tests were also conducted with seawater dilutions of 5, 10, 20, 50 and 100 times. These correspond to TDS around 9000, 4500, 2250, 900 and 450 ppm. The results (Figure 3) look similar to successful brines tested above. The ratios of ions in the diluted brines remain the same as SW however the ionic strength decreases by the dilution factor. The same mechanisms suggested above can be applied here, but now straight calcite dissolution may also occur if the brine is dilute enough that the Ca^{2+} concentration is below the saturation point. These results again agree with those of Zhang et al. (2012).

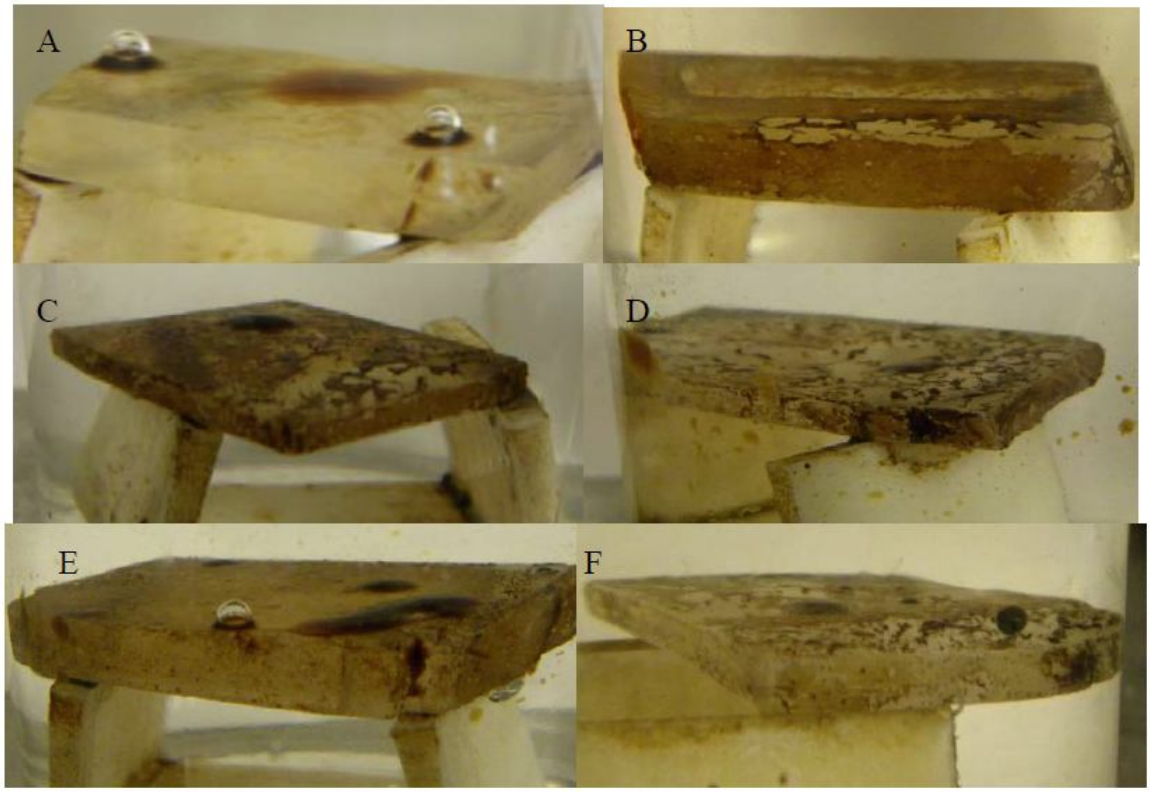

Figure 4-4: Calcite plate contact angle experiments with A) SW and dilutions of SW B) 5, C) 10, D) 20, E) 50 and F) 100

Figure 4-4A shows that SW composition brine also gave successful wettability alteration of the mineral plate, in line with the observations above. These results supported further investigation by spontaneous imbibition experiments.

Zhang & Sarma (2012) performed a similar study for a carbonate reservoir oil and rock at 90^{o}C. Their formation brine had a higher salinity level but contains less Mg^{2+} and SO_4^{2-}; the seawater brine composition was identical. Their results were very similar to those obtained here: sulfate was a potential determining ion and the mechanism of Zhang et al. (2007) was suggested in the presence of either divalent cations. MgCa4S gave the greatest wettability change to water-wet for their system.

4.3 SPONTANEOUS IMBIBITION

4.3.1 Modified Brine & Seawater Dilution

Spontaneous imbibition has long been used to evaluate rate and extent of wettability alteration. Table 4-3 lists the spontaneous imbibition tests, cores used (reservoir B), and summarizes the results. The experiments were conducted at 120°C. The brines chosen were based on the successful contact angle experiments seen above: Mg0Ca0S was chosen to see any effect of Mg^{2+} in isolation as was 0Mg0Ca4S for SO_4^{2-}. MgCa4S was also tested as it gave the smallest oil drops with the seemingly most water-wet contact angles, and SW/50 was chosen since all dilutions gave clean calcite plates and this brine has may be dilute enough (~800 ppm) to induce dissolution. The cores are somewhat heterogeneous; so raw data is presented in Figure 4-8, but is supplemented with Figure 4-9, which shows the time scaled according to Mattax & Kyte (1962). More applicable scaling techniques have been studied, but this scaling method was convenient to use.

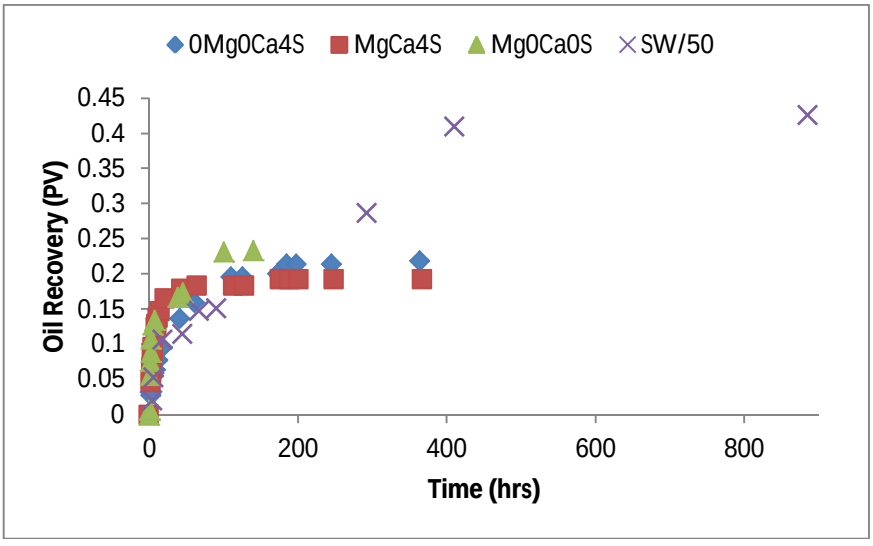

Figure 4-8: Imbibition behavior, raw fata of oil recovery in pore volumes against the time taken

Core	Brine	Recovery (PV)	Approximate Time (hrs)
Imb L10	Mg0Ca0S	0.23	100
Imb L8	MgCa4S	0.19	65
Imb L9	0Mg0Ca4S	0.22	100
Imb L11	SW/50	0.43	450

Table 4-3: Summary of brines tested in spontaneous imbibition experiments at 120C

Figure 4-8 shows that imbibition oil recoveries of the modified brines were very similar (approximately 0.2 PV) while that for the SW/50 dilution brine was much larger, 0.4 PV (pore volume). Mg0Ca0S and 0Mg0Ca4S each took around 100 hours to reach their maximum recovery, while MgCa4S took less time (65 hours). SW/50 took a significantly larger time of 450 hours; oil recovery was slow but continuous through this period. Out of the modified brines, 0Mg0Ca4S was the slowest, while MgCa4S and Mg0Ca0S recovered oil at a similar rate. Figure 4-9 clarifies the differences in recovery rates: 0Mg0Ca4S was the slowest, MgCa4S was slow to start but sped up later, and Mg0Ca0S had the fastest recovery rate throughout.

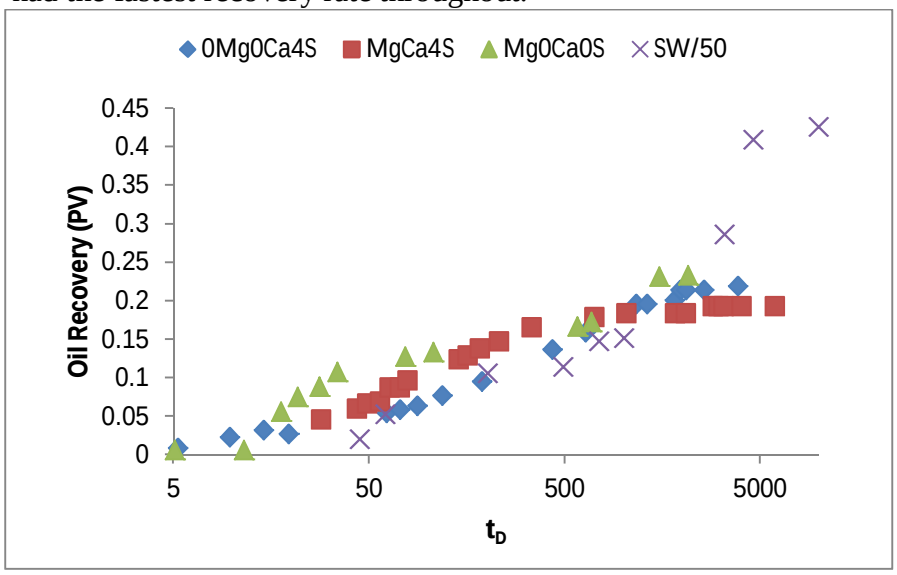

Figure 4-9: Imbibition behavior with Mattax & Kyte scaling with L equal to the core length

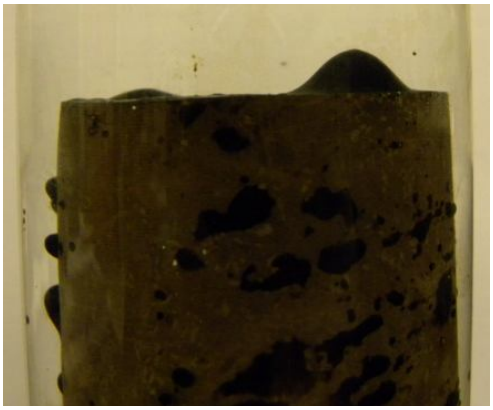

Figure 4-10: Image of oil recovery from core Imb L9 used with brine 0Mg0Ca4S

The wettability alteration mechanism associated with Mg0Ca0S brine may be dolomitization which is a fast process as it just depends on the Mg^{2+} availability and the size of the electrical double layer (Fathi et al., 2010, 2012). 0Mg0Ca4S brine's wettability altering mechanism is thought to be the multi-ion exchange process and is also the slowest as there is little divalent cation available (only that from the connate brine) to help the sulfate compete with the organic acid group. MgCa4S should follow the mechanism of Zhang et al. (2007) and the surface dolomitization process, but there is not enough information to prove this; the fast rate may be an indicator of both mechanisms occurring without rate limiting factors.

The slow and continuous nature of SW/50 recovery may indicate the dissolution mechanism. This may be triggered by the low ionic strength (small double layer) of the brine or it may be due to the very low divalent ion concentrations; it is not possible to distinguish between the two with these results. Ion analysis of flow experiments may reveal more information or show what material dissolves. This slow rate of recovery was also seen by Zhang and Sarma (2012) when they tested SW/40 at 70^{o}C. Their core was tighter at 1.1 md; thus the experiment was terminated after 50 days and only18% oil was

recovered. At 70°C dolomitization is unlikely to occur and any oil recovery indicates wettability alteration by low salinity dissolution.

4.4 CORE FLOODS & ION ANALYSIS

4.4.1 Modified Brine

The core floods presented here were performed at the reservoir temperature (120°C) with a back pressure of 50 psi; pressure is thought to have little impact on recovery behavior. The effluent brine from core floods was isolated and characterized for pH and ion concentrations using an ion chromatograph. Na^+, Cl^-, Ca^{2+}, Mg^{2+} and SO_4^{2-} concentrations were obtained to provide evidence for postulated mechanisms. The ion chromatograph can analyze brines up to a concentration of 4000 ppm; thus brines for analysis were first diluted.

4.4.1.1 Formation Brine – Base Case

Core CF B1 was used in a formation brine flood in order to have the base case recovery information. The core was flooded at a rate of 1 ft/day (0.045 ml/min). Figure 4-11 shows the recovery of 40% OOIP. The initial oil saturation is 68% and water flooding decreases oil saturation to 41% by about 5 pore volumes injected. The pressure drop is also shown and it follows the expected trend. The pH starts around 5 and increases gradually to stabilize at approximately 6.4, which is the pH of the formation brine. The initial pH is expected to be low because the aging of the oil and brine with the rock leads to ion exchange of organic acids and release of H^+ ions. The core-equilibrated brine is recovered first followed by the freshly injected brine of the water flood. Early oil water breakthrough and slow recovery are more indications of an initially oil-wet core.

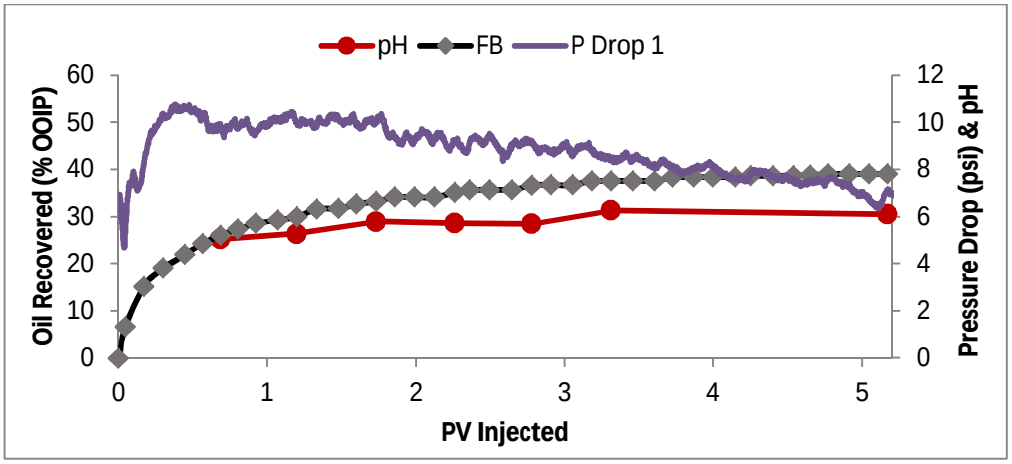

Figure 4-11: Formation brine base case flood showing oil recovery, pH and pressure drop

Figure 4-12 shows the continuation of the previous flood: the FB flood rate was increased by 10 times (10 ft/day) until recovery stabilized, followed by modified brine MgCa4S. An additional 7% recovery from the high rate flood can be due to two effects: a) the effect of increasing the capillary number by one order of magnitude which leads to the reduction of the residual oil saturation, and b) the decrease in the capillary end effect due to the high rate flood. Capillary end effect is possible due to the small core length. If it is a heterogeneity effect, it suggests residual oil saturation variation with the capillary number. An estimate of the capillary number for the low rate flood has order of magnitude 10^{-6} which becomes 10^{-5} for the high rate flood; Kamath et al. (2001) report such effects for carbonate rocks. An example (Figure 4-13) of the desaturation curves confirms a reasonable capillary number magnitude, and S_{or} dependence, (core CF B1 data superimposed in orange). The core most closely matches sample K5 from Kamath et al. (2001) which was characterized as a heterogeneous compound limestone, mega-macroport rock with significant microporosity, and fairly large pore body-throat aspect ratio. An additional note for this flood is that the pressure drop does not increase ten times with a ten times increase in flow rate.

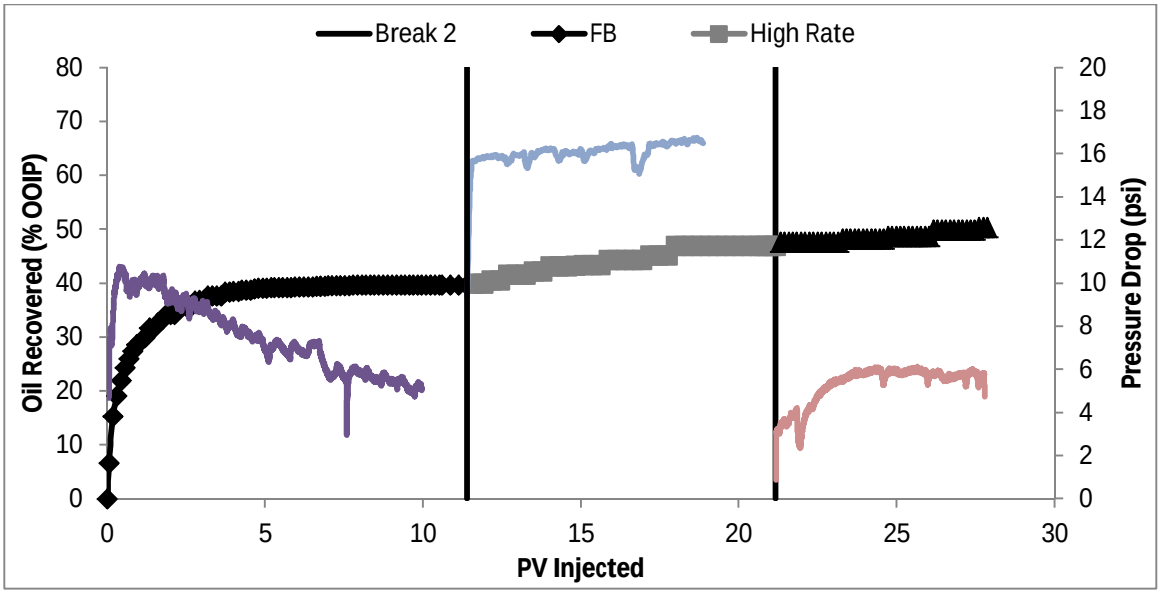

Figure 4-12: FB followed by high flow rate FB and MgCa4S brine as 3rd injection fluid

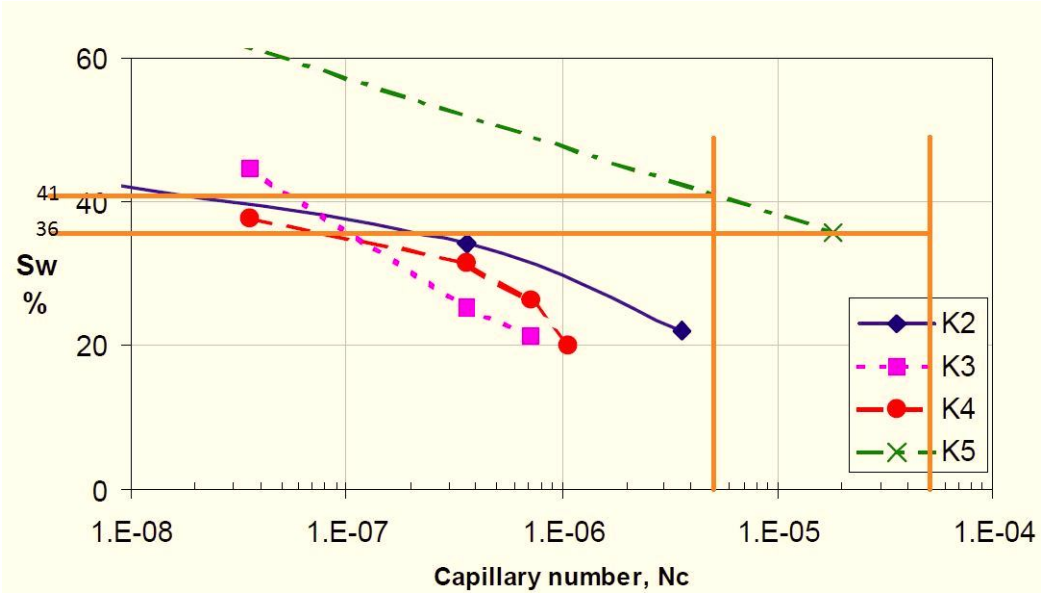

Figure 4-13: Experimental capillary desaturation curves (Kamath et al., 2001); Core CF B1 data represented by solid orange lines.

CaMg4S is the third injection fluid at 1 ft/day flow rate. Even with successful wettability alteration on the calcite plate and imbibition core, very little extra oil is

produced over the high rate FB flood. This observation may not prove that CaMg4S is not a wettability-altering agent. Assuming an oil-wet core, formation brine invades and exists in intermediate and larger pores after the high rate rate waterflood while the smaller pores are still filled with oil. In changing flow rates from 10 ft/day back to 1 ft/day perhaps oil closes off some small pore throats again and the modified brine does not even contact the pore-wall of small pores for higher oil recovery. CaMg4S flood is tested later in the secondary mode.

The ionic composition of the effluent brine is plotted in Figure 4-14. The dashed lines in the figure correspond to the injected concentrations of the ions, i.e., FB concentrations. The effluent brine concentration is not exactly the same as that of the injection brine; the ion concentrations are higher in the effluent up to 1 PV injection, except for Cl- which is lower by a factor of 5. After 1 PV injection, Na^{+}, Ca^{2+} and SO_4^{2-} concentrations return to the injection brine level, but the Mg^{2+} concentration remains low, diluted to one-third the injection concentration. The results indicate that there is some dissolution and/or release of cations during aging. The SO_4^{2-} is also released and possibly displaced by organic acids of the oil. The chloride may have replaced some ions in the diffuse and immobile layers. After the injection brine breaks through, some SO_4^{2-}, Ca^{2+} and Mg^{2+} are re-adsorbed to the rock surface (since their concentrations are below injection levels). Na^{+} returns to the injection level, while $SO_4^{2-}$and Ca^{2+} return close to injection concentrations. Mg^{2+} continues to be very strongly adsorbed as does Cl^{-}.

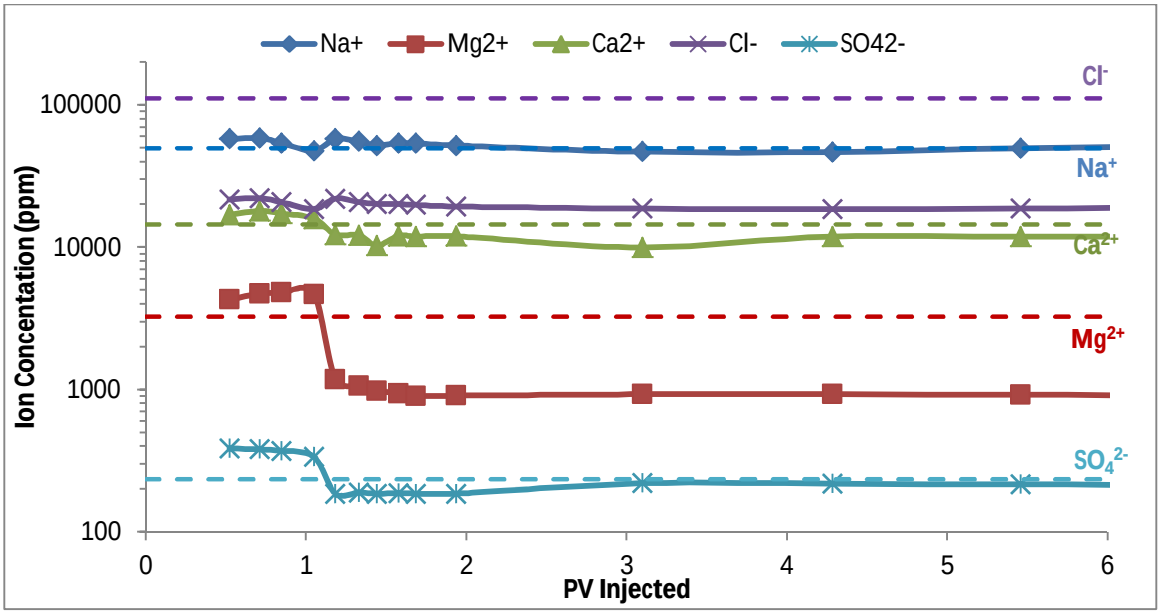

Figure 4-14: Effluent ion composition of formation brine flood

4.4.1.2 CaMg4S Wettability Altering Brine

MgCa4S was injected to evaluate secondary recovery in core CF B2. The result shows a very high recovery of 76% OOIP after around 4.5 pore volumes of brine injected (Figure 4-15). The graph indicates a jump in the recovery at the end of the modified brine (MB) flood, but this is simply an effect of the back pressure regulator releasing collected liquid. The pressure profile is as expected, although the gradient is greater than 1 psi/ft. This experiment was repeated in core CF B3 (data not presented here) to confirm the success of this brine, which yielded a similarly high value of oil recovery even in a lower permeability core.

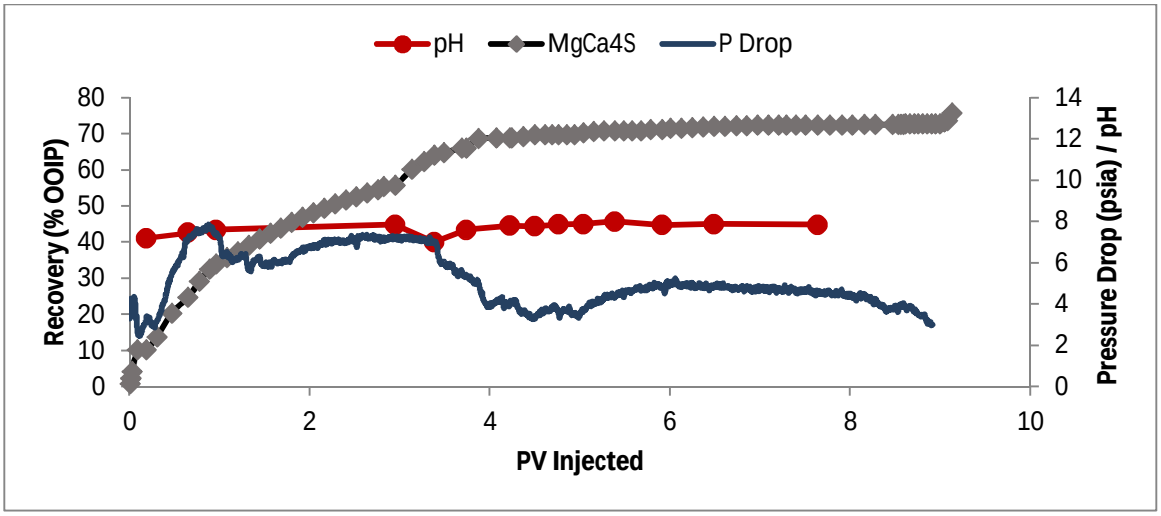

Figure 4-15: CaMg4S brine flood 2^{o} recovery mode showing oil recovery, pH and pressure drop

The pH of the effluent brine is initially close to 7, later increasing to an equilibrium value of 7.8. The acting mechanism is suggested to be multi ion exchange (Zhang et al., 2007) and the pH corroborates this. The modified brine is expected to carry lower pH as the extra sulfate concentration would cause more water dissociation and free hydrogen ions. During ion exchange with the modified brine, the acid groups leave the rock surface pairing with divalent cations, leaving free chloride and sulfate anions in solution which complex with free H^+ to decrease the free H^+ concentration, raising the pH to slightly alkaline conditions.

The effluent from this core flood was also analyzed for ion behavior. In Figure 4-16, the ion concentrations are normalized against the injection brine composition, e.g., the Na^+ concentration was normalized by the Na^+ content of the injection brine, which is 49,933 ppm from Table 3-1. The orange dashed line thus shows the injection slug concentrations of the ions, i.e., the value is 1. Figure 4-16 shows that Ca^{2+}, Na^+, and Cl^- drop to injection brine levels in 2-3 PV injected, and Ca^{2+} drops further settling at half the

injection concentration. Mg^{2+} and SO_4^{2-} remain at half the injection slug concentration. These trends fall exactly in line with the mechanism from Zhang et al. (2007); it explains why the Mg^{2+} and SO_4^{2-} concentrations seen in the experiment's effluent are much lower than the injection slug concentrations. This change in ion potential and adsorbed components change the wettability of the rock surface and promote further imbibition of water, giving the end result of improved oil recovery from a formation brine waterflood. The result differs from that of Vo et al. (2012) where Ca^{2+} is the only ion that does not change to injection brine concentrations and dissolution was the suggested mechanism.

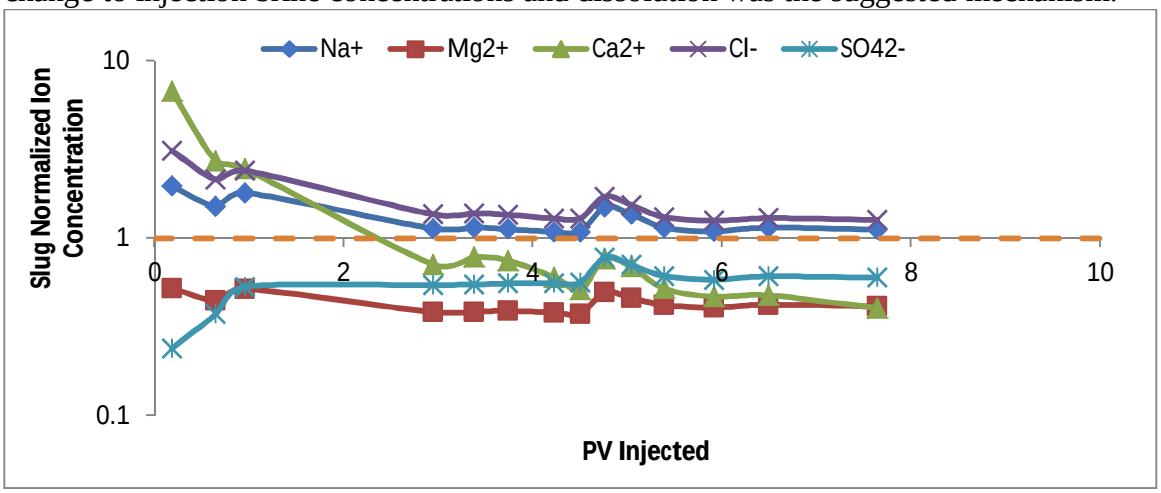

Figure 4-16: Effluent ion analysis for CaMg4S secondary mode flood

Alternative Oxidizing Agent: Figure 4-17 below shows injection of persulfate and dichromate rich brines after the high oil recovery by CaMg4S brine; however, too small a volume of oil was recovered to draw any conclusion. As before, this does not rule out wettability altering ability of the brines since little oil remained available for recovery after the CaMg4S flood.

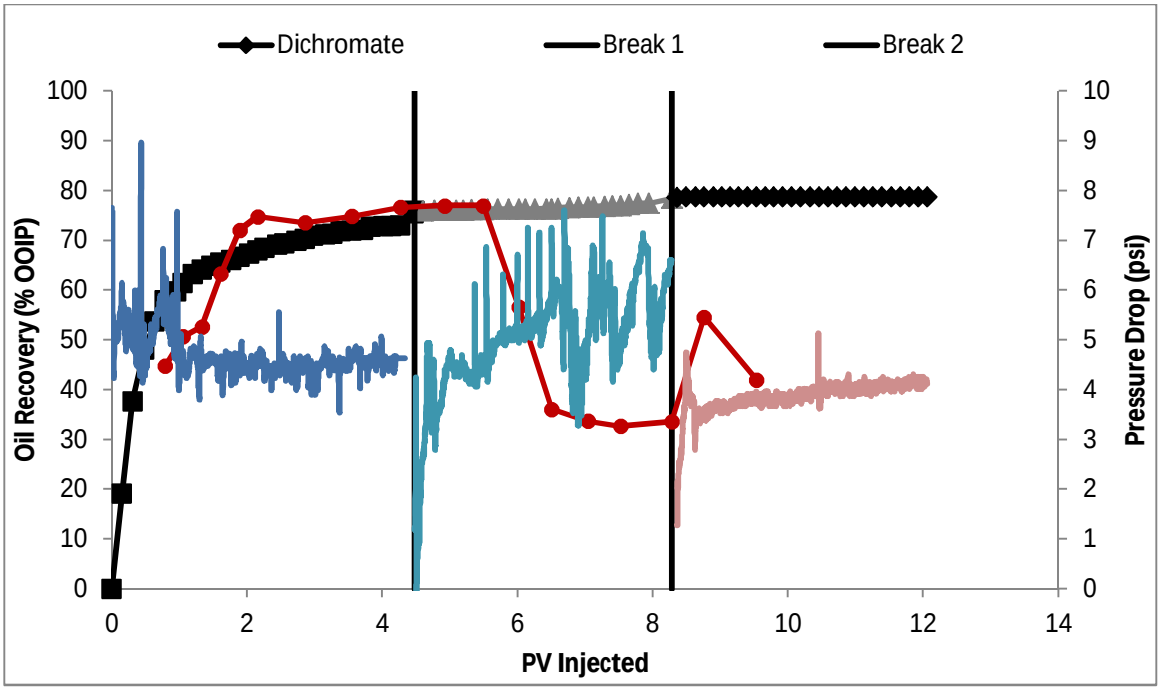

Figure 4-17: CaMg4S flood (same as previous) with alternative oxidizing agent brines injected next

4.4.1.3 Reservoir A – 0Mg0Ca4S Flood

A tighter core from reservoir A was used to test a successful brine based on contact angle tests with oil A: 0Mg0Ca4S. The water flood with FB-A gave poor recovery around 20% OOIP in 3 PV injected, although the pressure drop was small in comparison to those seen for rock B. The tertiary mode injection of 0Mg0Ca4S gave incremental oil recovery of 15% OOIP, but the overall efficiency is still poor and the pressure drop does not indicate the pushing of a large oil bank. Improved tuning and screening of injection brine is required for this COBR.

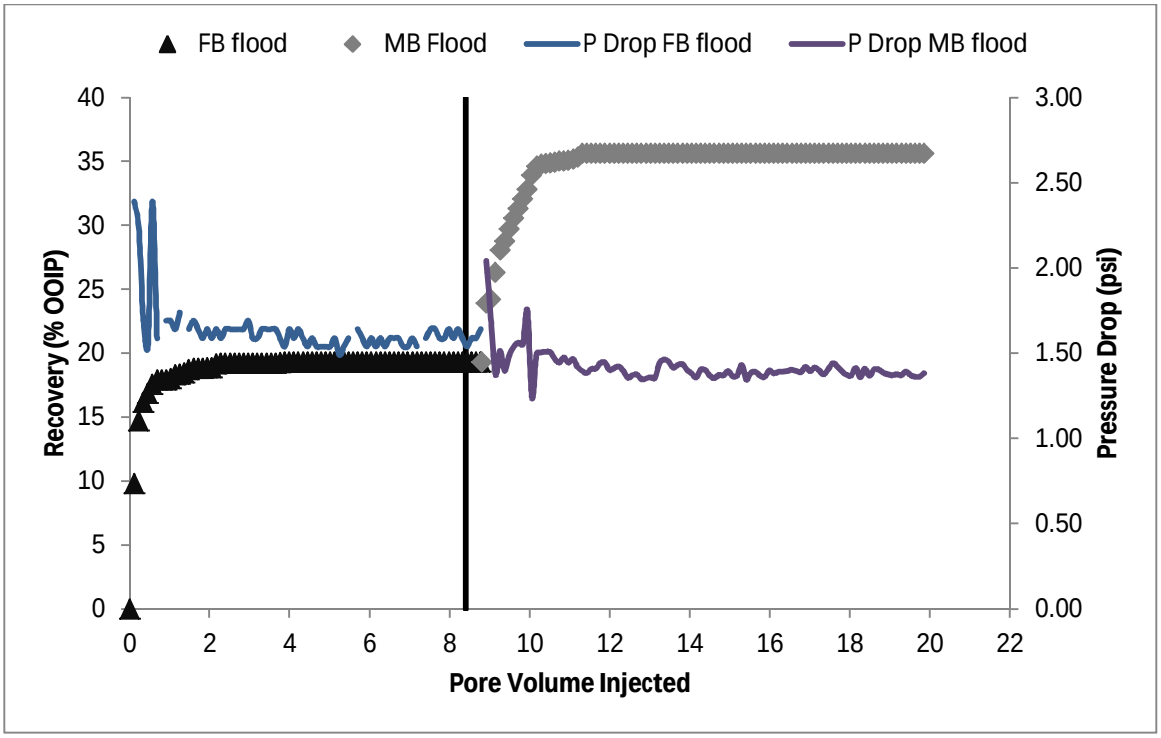

Figure 4-18: 0Mg0Ca4S modified brine in the tertiary mode for reservoir A

4.4.2 Seawater Dilution

4.4.2.1 Sequential Dilution of Sea Water

Yousef et al. (2010) showed the utility of diluted seawater floods. This process was imitated in core CF B4 for our rock-oil system and Figure 4-19 shows oil recovery in the SW core flood. Seawater gave a recovery of 47% OOIP after 5 PV injected. This recovery is higher than the formation brine waterflood above, which yielded 40% OOIP. The pressure drop had a lot of fluctuation due to the malfunction of the back pressure regulator, but the magnitude is similar to the pressure gradients of previous floods. The pH increased from 6.7 to 7.7 as the SW brine is injected. The injected SW pH was 6.9; so there was a significant increase and this behavior is similar to that of CaMg4S flood. The

flow rate was increased to 10 ft/day to check for capillary end effect, but no extra oil was recovered in 2 PV injection.

The next slug was SW/2 at half the sea brine salinity. This brine recovered an extra 10% OOIP within 3 PV injected, with a similar pressure drop to the SW flood. The rate increase in this case recovered significant oil (15% OOIP). End effect was ruled out in the first slug, and assuming the same here, the twice diluted SW may be causing dissolution effects, perhaps indicating a threshold salinity (between 43,000 ppm and 21,500 ppm) below which this mechanism begins. The pH decreased to 7.4 and remained steady.

SW/10 was injected next and able to recover some remaining oil (3% OOIP) after which no more oil is produced even with a flow rate increase and a brine composition change. This likely indicates reaching the residual oil saturation to brine. The pH increased to 7.9 and remained steady.

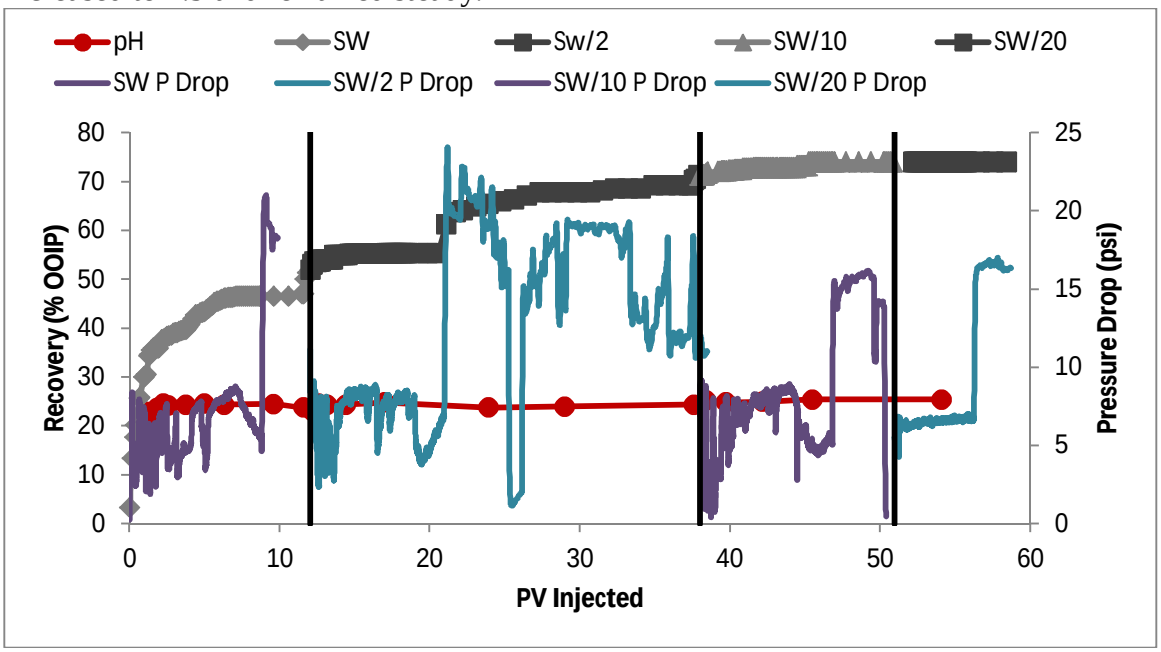

Figure 4-19: SW and dilutions sequential flood

The effluent ion composition (Figure 4-20) is quite different from that seen in the CaMg4S flood. In this case, the Na^+, Cl^- and SO_4^{2-} ions settle around the normalized concentration value of 0.85, while Mg^{2+} ions remain low at 0.5 and Ca^{2+} is at 1.2 times the SW slug. The dolomitization mechanism explains this result where Mg^{2+} substitutes out Ca^{2+} at the rock surface under high temperature. As the Mg^{2+} attaches to the surface, the surface or diffuse layer SO_4^{2-} content may become larger, holding additional Mg^{2+} in these layers as well. Consequently Mg^{2+} content of the effluent brine is much lower than that of the injection brine; the Ca^{2+} is greater and the SO_4^{2-} is less. The multi ion exchange mechanism is not suggested here because the sulfate concentration does not decrease enough.

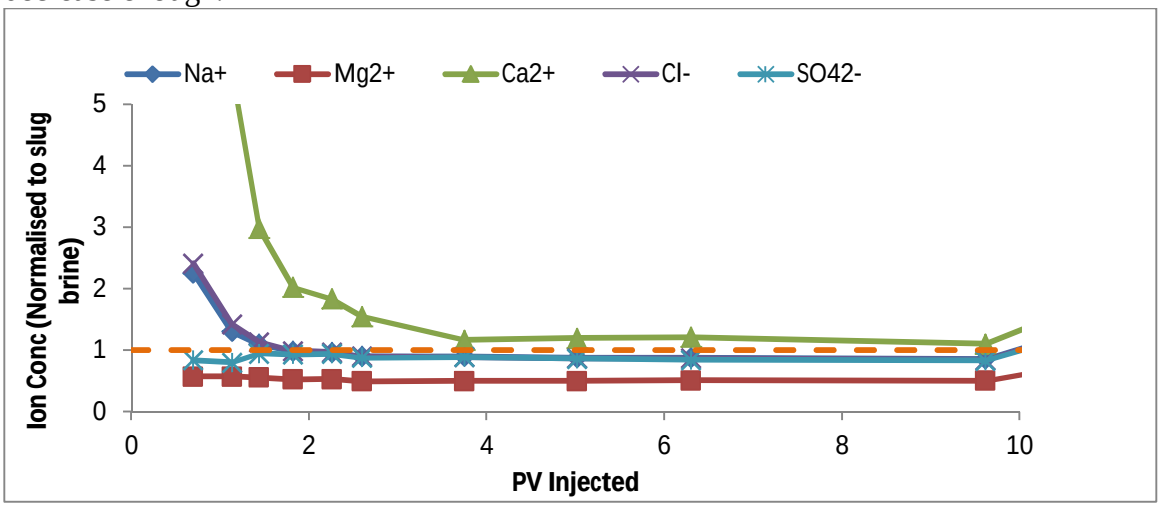

Figure 4-20: SW slug ion analysis

The SW/2 slug shows similar ion behavior to that of SW (figure 4-21). The first point simply shows the adjustment to the half concentrations of each ion, but the Mg^{2+} and SO_4^{2-} are again below injection levels, and Ca^{2+} is above injection level. In the SW slug, effluent Ca^{2+} was at 1.15 times the injection concentration, whereas it is 1.3 times the injection concentration for this SW/2 slug. The rate change does not affect other ion concentrations noticeably.

Figure 4-22 shows the ion concentrations for the next two slugs (SW/10 and SW/20). The non-potential determining ions (Na^+, Cl^-) and Mg^{2+} ratios remain the same with respect to the injection brine. However, the SO_4^{2-} concentration rises to approximately 1.25 times the injection concentration, and Ca2+ is now much larger than injection levels (~3 times greater). This is an indication of the dissolution mechanism.

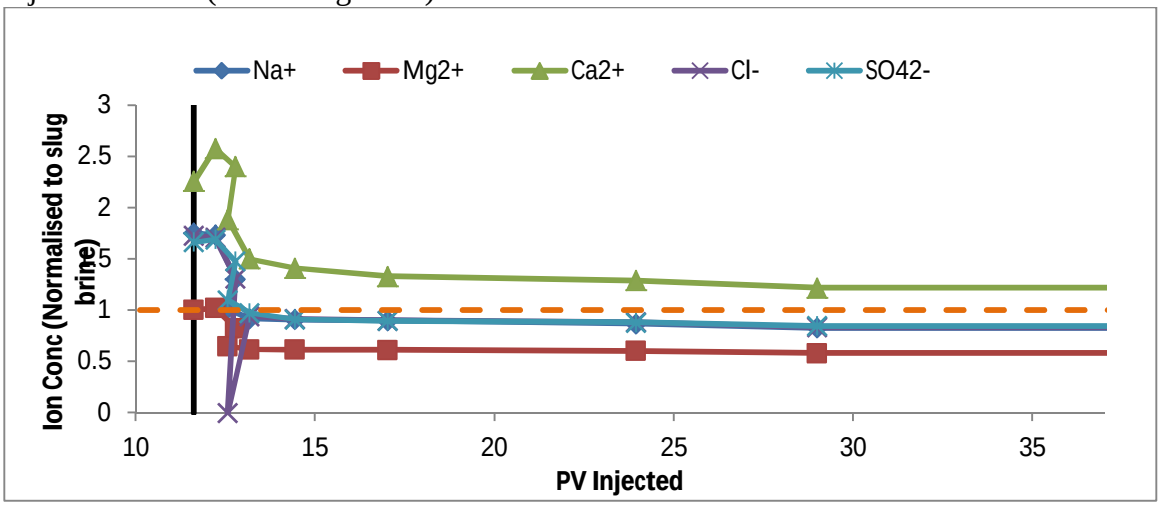

Figure 4-21: SW/2 slug ion analysis

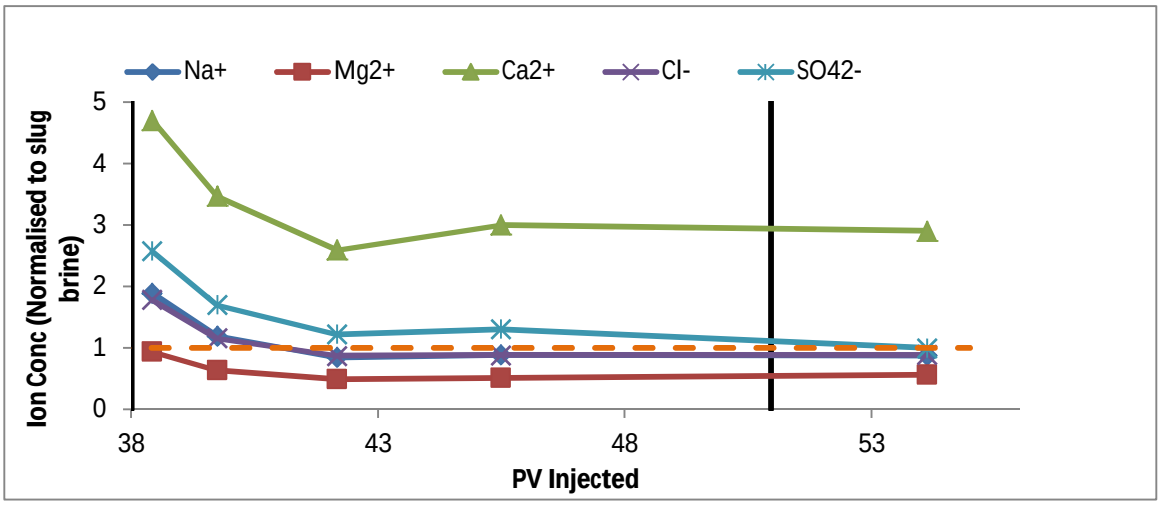

Figure 4-22: SW/10 and SW/20 slug ion analysis

4.4.2.2 SW/50 in Tertiary Mode

The strong imbibition performance of diluted seawater SW/50 led to further investigations. Core CF B5 was first water flooded with FB, followed by SW/50 in the tertiary mode. The FB flood recovered just over 40% OOIP (Figure 4-23) as before and the diluted seawater gave an incremental recovery of 32% OOIP yielding 72% OOIP oil recovery in total. The pH shows an increase during the water flood from 5.2 to 6, and a further increase to 7.5 during tertiary recovery (the end point is similar to SW and MgCa4S floods). The pressure drop is not shown here; it is similar to the pressure profile of the modified brine flood (CaMg4S).

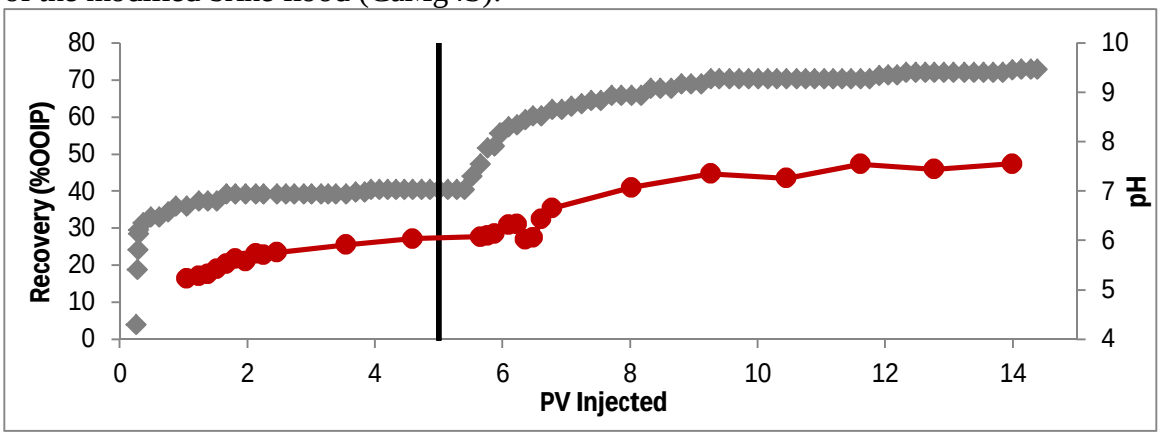

Figure 4-23: 50x diluted SW tertiary flood showing oil recovery and pH

The ion analysis is shown in Figure 4-24; the dashed lines in this chart show the ratio of concentrations in FB and SW/50, for each ion, and are meant to give a more clear view of the concentration drop of the ions. The FB flood results are not shown as they are very similar to those of flood 1; only results from 5-14 PV injected (SW/50 section) are presented. The ion concentration ratios at 5 PV are larger than in previous plots, since formation brine is almost 200 times more concentrated than SW/50. All normalized concentrations are expected to drop to 1 if no reaction, dissolution or ion exchange were to occur.

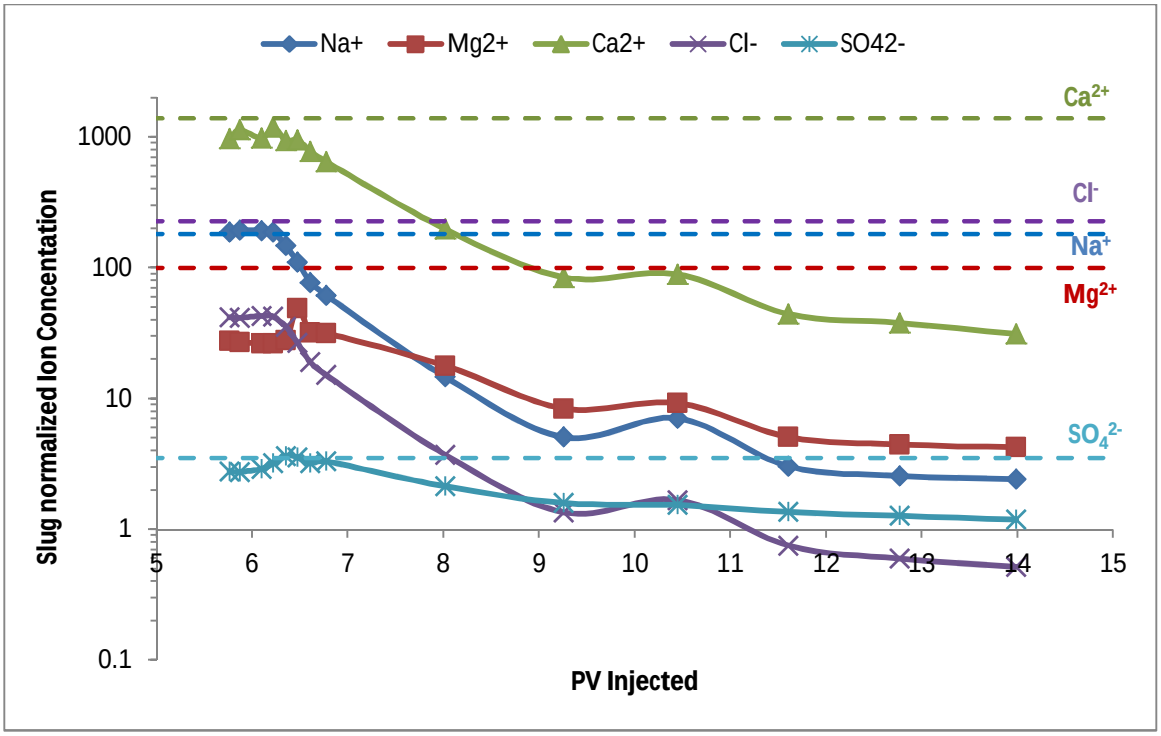

Figure 4-24: Effluent ion analysis of 50x diluted SW in tertiary mode

4.4.2.3 SW/20 in Tertiary Mode

SW/20 in the tertiary mode behaves almost identically to the SW/50 tertiary flood giving slightly higher oil recovery of 80%. The pH and effluent ion behavior are also comparable. There is no indication of dissolution rate differences between the two floods.

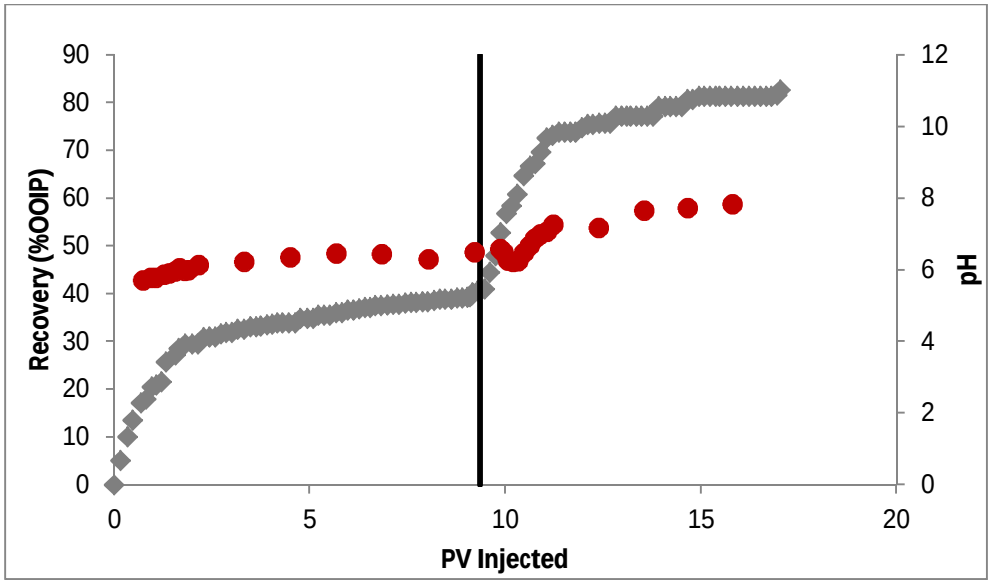

Figure 4-25: 20x diluted SW tertiary flood showing oil recovery and pH

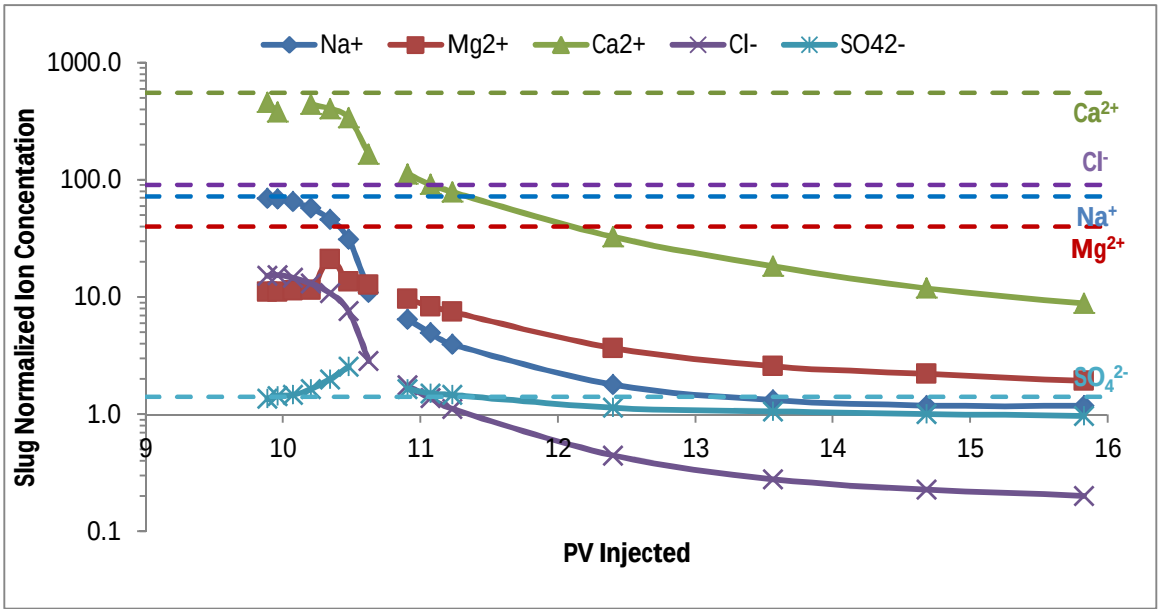

Figure 4-26: Effluent ion analysis of 20x dilution SW in tertiary mode

4.4.2.4 SW/50 in the Secondary Mode

SW/50 is injected in the secondary mode to observe any changes in recovery from the tertiary mode and to see if ion behavior can give further insight into mechanisms.

Similar to the tertiary mode, many PVs were injected (19) to reach the final recovery of 85% OOIP (Figure 4-27). The overall performance is the best out of all five floods even though it is the slowest process. The pH rises from 6 to 7.3. The ion analysis is shown in Figure 4-28 (read similarly to Figures 4-24 and 4-26) and shows the simplest behavior of all the floods: the concentrations monotonically decrease, but not to the injection level.

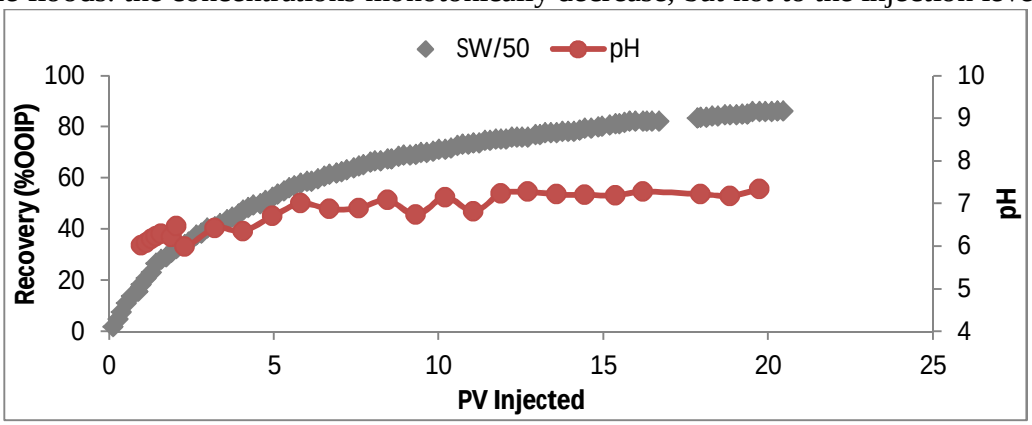

Figure 4-27: Secondary mode 50x diluted SW flood showing oil recovery and pH

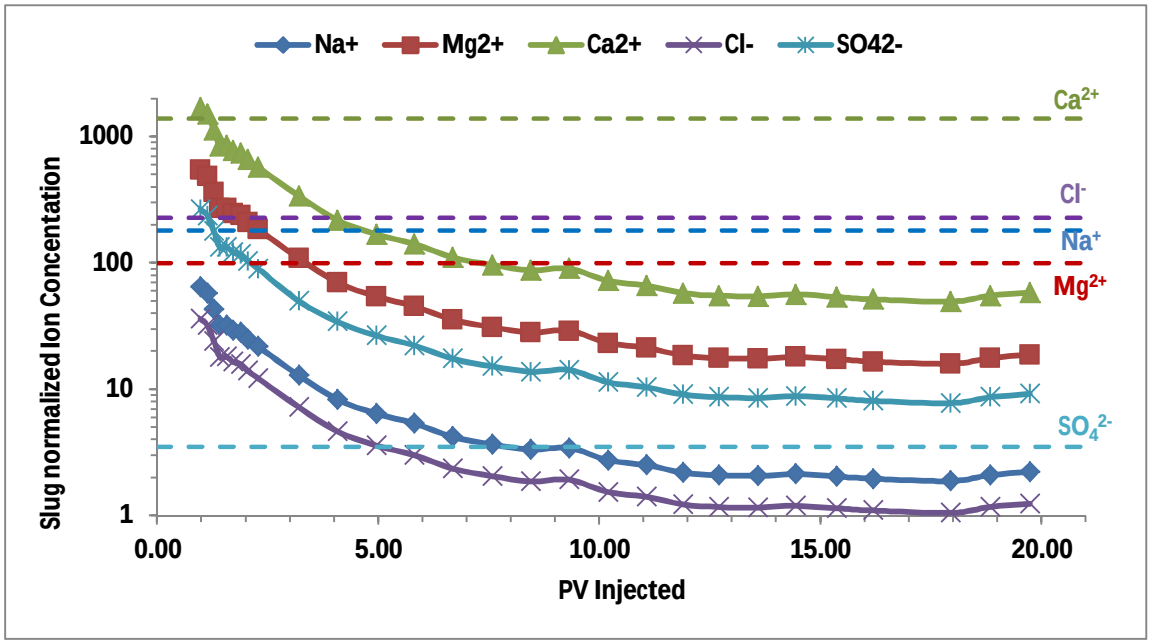

Figure 4-28: Effluent ion analysis of secondary mode 50x dilution SW flood

4.4.2.5 SW/20 in the Secondary Mode

SW/20 recovered 65% OOIP in the secondary mode (core CF B6), but in fewer pore volumes injected than for SW/50. The effluent ions also drop closer to the injection level concentrations, probably indicative of the weaker dissolution.

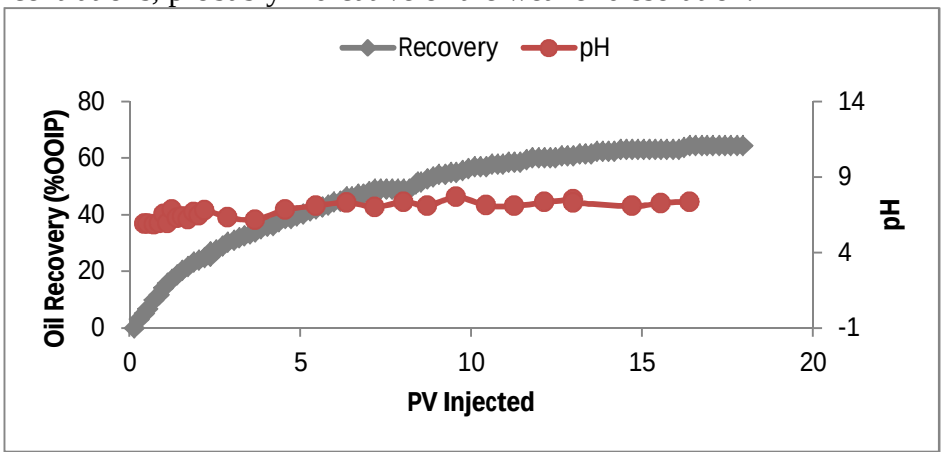

Figure 4-29: Secondary mode 20x diluted SW flood showing oil recovery and pH

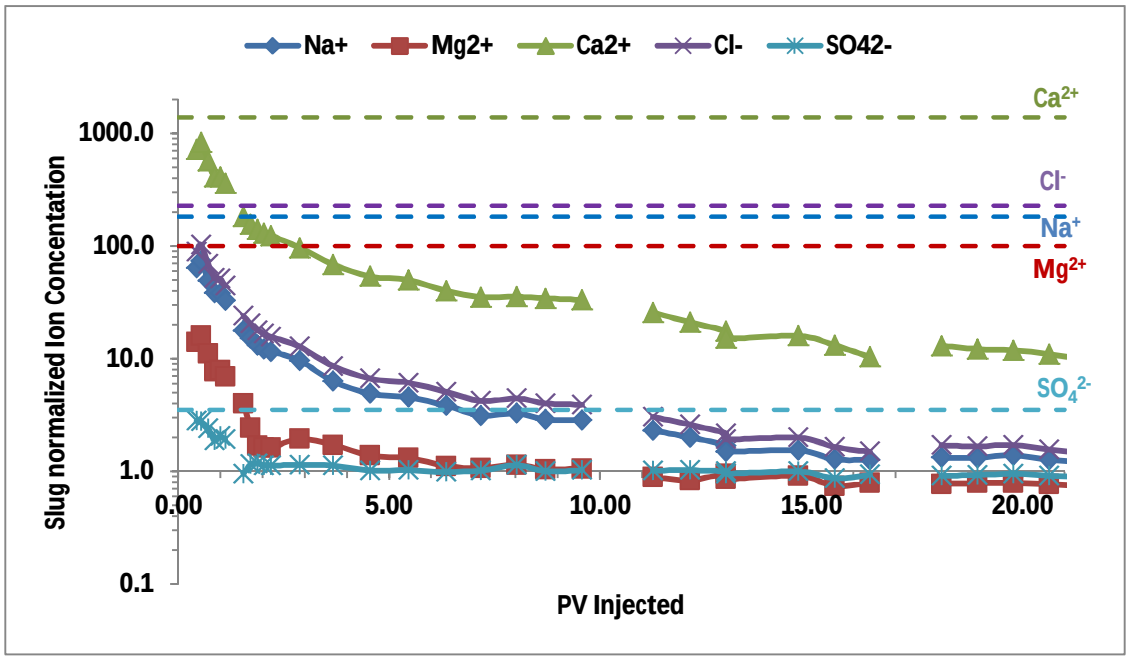

Figure 4-30: Effluent ion analysis of secondary mode 20x dilution SW flood

4.4.2.6 Comparing secondary and tertiary modes

The discussion here deals with SW/50 in the secondary and tertiary modes, but the principles apply the comparison of SW/20 in the secondary and tertiary modes. The starting concentrations in the secondary and tertiary floods both agree with the ion concentrations seen in the formation brine base case flood, i.e., a difference between the connate (or equilibrated) FB and the fresh FB is observed. For the SW/50 cases, Na^+ and Cl^- concentrations decrease close to the injection concentration and seem inactive, but Ca^{2+} reaches around 30-50 times the SW/50 concentration in about 15 PV injected. This Ca^{2+} concentration is high enough to consider it as a symptom of core surface dissolution. Mg^{2+} also decreases monotonically stabilizing between 5x and 20x of the injection concentration, which may be explained by a small surface dolomite dissolution. Austad et al. (2012) proposed that anhydrite is a necessity for dissolution to occur, and the results of the secondary mode may support this proposition, but SO_4^{2-} concentration in tertiary mode reaches the injection brine concentration indicating the absence of anhydrite dissolution. Vo et al. (2012) also suggested that dissolution may cause fluctuations in the pressure drop if large particles of rock are released or precipitation of certain salts blocking flow paths; such conclusions cannot be made in this case as the back pressure regulator has behaved unreliably in the past.

The secondary and tertiary mode oil recoveries are similar to the yields from experiments by Yousef et al. (2010). The difference in recoveries between these two modes is attributed to the fact that water flood creates a flow path and the tertiary SW/50 flood does not sweep as large a volume as it does in the secondary mode. Additionally, the tertiary mode injection means the SW/50 must displace a much larger volume of FB in front of it than it does in the secondary mode. These floods and the modified brine

flood gave similar oil recovery indicating that the residual oil saturation to these wettability altering brines seems to be around 18-20.

The ion analysis results provide evidence for the postulated mechanisms: multi ion exchange, bulk mineral dissolution, and surface dissolution. Some of the ion behavior, such as low Cl^- ions in FB flood or the change in concentrations between fresh FB and the connate brine, is not fully understood and requires further study and modeling. A fundamental problem with ion analysis of effluent brine is the change in temperature between the coreflood and the ion analysis equipment. As the aqueous samples cool and as they are exposed to atmospheric CO_2, Ca^{2+} concentrations may change due to the reaction equilibria of Ca^{2+}, CO_3^{2-} and HCO_3^- ions among others. Better post processing of the effluent brine may be required to mitigate this effect.

The scale-up of the ion exchange and mineral dissolution mechanisms are different. The ion exchange and surface (or any limited) dissolution mechanisms can be propagated through the whole reservoir, but bulk dissolution may not be. The injected brine will get saturated with the dissolving mineral within some distance into the reservoir and there would be no dissolution in the further downstream part of the reservoir. If the wettability alteration solely depends on the bulk dissolution mechanism, one can see a significant enhanced oil recovery in a core, but not in a reservoir. Further tests need to be conducted in longer cores and models need to be developed for proper scale-up of these processes.

Chapter 5: Conclusions & Further Work

The effect of brine ionic composition on oil recovery was studied for a limestone reservoir rock at 120°C. Contact angle, Amott imbibition, core flood, and ion analysis were used to find the brines that improve oil recovery and the associated mechanisms. The findings of this study are listed here along with suggestions for future work.

5.1 CONCLUSIONS

1) Contact angle experiments showed that modified seawater containing Mg^{2+} and SO_4^{2-} and diluted seawater change oil-wet calcite plates to more water-wet conditions. Presence of Ca^{2+} without Mg^{2+} or SO_4^{2-} was unsuccessful in changing calcite plate wettability.
2) Mg^{2+} and SO_4^{2-} are the key potential determining ions.
3) Modified seawater containing Mg^{2+} and SO_4^{2-} and diluted seawater spontaneously imbibe into the originally oil-wet limestone cores.
4) Modified seawater containing extra SO_4^{2-} and diluted seawater (20 and 50 times) improve oil recovery from 40% OOIP (for formation brine waterflood) to about 80% OOIP in both secondary and tertiary modes. The residual oil saturation to modified brine injection is approximately 20%.
5) Multi ion exchange and mineral dissolution are responsible for desorption of organic acid groups which lead to more water-wet conditions.

5.2 FURTHER WORK

Wettability alteration by low salinity brine is influenced by many parameters that are not yet fully understood. Possible extensions to the work are listed here:

- Changing core dimensions may alter overall oil recoveries depending on kinetics of ion exchanges and mineral dissolution.

- Varying flow rate would also affect the mechanisms involved and add understanding to model scale up to reservoir dimensions.
- The ratio of specific ions at different salinity levels will certainly affect the dissolution and ion exchange mechanism, perhaps allowing higher quality results to model using thermodynamic engines like PHREEQC
- Investigation of salinity versus recovery could yield an optimum injection brine composition.
- CO_2 interaction with low salinity brine may be explored for EOR purposes.
- For a fundamental understanding of the wettability altering potential, DLVO theory models may be used to predict brine thin film thicknesses and the potential of any given brine or crude oil of known TAN to alter wettability.
- More appropriate scaling groups for spontaneous imbibition experiments should be considered.
- Capillary pressure curve and relative permeability should be measured as a function of brine composition, perhaps linking them to contact angle results.
- Chemical scale issues may occur with these brine compositions at the reservoir scale, and should be studied.

References

Abdullah, W., Buckley, J.s., Carnegie, A., Edwards, J., Herold, B., Fordham, E., Graue, A., Habashy, T., Seleznev, N., Signer, C., Hussain, H., Montaron, B., and Ziauddin, M. 2007. Fundamentals of Wettability. Schlumberger Oilfield Review **19** (2): 44-61.

Anderson, W.G. 1986. Wettability Literature Survey-part 1: Rock/Brine/Oil Interactions and the Effects of Core Handling on Wettability. Journal of Petroleum Technology 38: 1125-1144.

Anderson, W.G. 1986b. Wettability Literature Survey-Part 2: Wettability Measurement. Journal of Petroleum Technology **38** (11): 1246-1262.

Austad, T., Strand, S., Hognesen, E.J. and Zhang, P. 2005. Seawater as IOR Fluid in Fractured Chalk. Paper SPE 93000 presented at the SPE International Symposium on Oilfield Chemistry, 2-4 February, Houston, TX.

Austad, T., Strand, S., Madland, M., Puntervold, T. and Korsnes, R. 2008. Seawater in Chalk: An EOR and Compaction Fluid. Journal of SPE 12 Reservoir Evaluation & Engineering: 648-654.

Austad, T., Strand, S., Madland, M. V., et al. 2009. Is Wettability Alteration of Carbonate by Seawater Cause by Rock Dissolution? Paper SCA 2009-43 presented at the International Symposium of the Society of Core Analysts, 27-30 September, Noordwijk, The Netherlands.

Austad, T., Shariatpanahi, S.F., Strand, S., Black, C.J.J. and Webb, K.J. 2012. Conditions for a Low-Salinity Enhanced Oil Recovery (EOR) Effect in Carbonate Oil Reservoirs. Energy & Fuels **26** (1): 569-575.

Baptist, O.C. and Sweeney, S.A. 1954. The Effect of Clays on the Permeability of Reservoir Sands to Waters of Different Saline Contents. Paper presented at Pacific Coast Regional Conference on Clays and Clay Technology, 25-26 June, Berkeley, CA.

Barnes, J. R., Dirkzwager, H., Smit, J. R., Smit, J. P. and On, A. 2010. Application of Internal Olefin Sulfonates and Other Surfactants to EOR. Part 1: Structure – Performance Relationships for Selection at Different reservoir Conditions. Paper SPE 129766 presented at SPE Improved IOR Recovery Symposium, 24-28 April, Tulsa, OK, USA.

BP. 2013. BP Statistical Review of World Energy, June 2013. http://www.bp.com/en/global/corporate/about-bp/statistical-review-of-world-energy-2013.html.

Buckley, J.S., Liu, Y., Xie, X., and Morrow, N. R. 1997. Asphaltenes and Crude Oil Wetting – The Effect of Oil Composition. SPE Journal, **2** (2): 107-119.

Chen, P. 2012. Surfactant-Enhanced Spontaneous Imbibition Process in highly Fractured Carbonate Reservoirs. M.S. Thesis. The University of Texas at Austin. Austin, TX.

Doust, A.R., Puntervold, T.P., Strand, S. and Austad, T.A. 2009. Smart Water as Wettability Modifier in Carbonate and Sandstone. Energy & Fuels, **23**: 4479-4485.

Fathi, S.J., Austad, T. and Strand, S. 2010. "Smart Water" as a Wettability Modifier in Chalk: The Effect of Salinity and Ionic Composition. Energy & Fuels **24** (4): 2514–2519.

Fathi, S.J., Austad, T. and Strand, S. 2012. Water-Based Enhanced Oil Recovery (EOR) by "Smart Water" in Carbonate Reservoirs. Paper SPE 154570 presented at the SPE EOR Conference at Oil and Gas West Asia, 16-18 April, Muscat, Oman.

Gupta, R.P., Smith, G.J., Hu, L., and Willingham, T.W., Cascio, M.L., Shyeh, J.J. and Harris, C.R. 2011. Enhanced Waterflood for Middle East Carbonate Cores – Impact of Injection Water Composition. Paper SPE 142668, presented at the SPE Middle East Oil and Gas Show and Conference, 25-28 September, Manama, Bahrain.

Hiorth, A., Cathles, L.M., Kolnes, J., Vikane, O., Lohne, A. and Madland, M.V. 2008. A Chemical Model for the Seawater-CO2-Carbonate System - Aqueous and Surface chemistry. Paper SCA2008-18 presented at the International Symposium of the Society of Core Analysts, 29 October – 2 November, Abu Dhabi, UAE.

Hirasaki, G. 1991. Wettability: Fundamentals and Surface Forces. Journal Paper SPE 17367, SPE Formation Evaluation **6** (2): 217-226.

Hirasaki, G. and Zhang, D.L. 2004. Surface Chemistry of Oil Recovery from Fractured, Oil-Wet Carbonate Formations. Paper SPE 88365 *SPEJ* **9** (2): 151–162.

Høgnesen, E.J., Strand, S., Austad, T. 2005. Waterflooding of Preferential Oil-Wet Carbonates: Oil Recovery Related to Reservoir Temperature and Brine Composition. Paper SPE 94166 presented at Europec/EAGE Annual Conference, 13-16 June, Madrid, Spain.

Jadhunandan, P.P. 1990. Effects of Brine Composition, Crude Oil and Aging Conditions on Wettability and Oil Recovery. Ph.D. Dissertation.

Jadhunandan, P.P. and Morrow, N.R. 1995. Effect of Wettability on Waterflood Recovery for Crude-Oil/Brine/Rock Systems. Journal Paper SPE 22597, SPE Reservoir Engineering **10** (1): 40-46.

Kamath J., Meyer, R. F., Nakagawa, F. M. 2001. Understanding Waterflood Residual Oil Saturation of Four Carbonate Rock Types. Paper SPE 71505 presented at SPE Annual Technical Conference and Exhibition, 30 September-3 October, New Orleans, LA, USA.

Kozaki, C. 2012. Efficiency of Low Salinity Polymer Flooding in Sandstone Core. Master's Thesis.

Lager, A., Webb, K.J., Black, C.J.J., Singleton, M., Sorbie, K.S. 2006. Low Salinity Oil Recovery - An Experimental Investigation. Paper SCA2006-36 presented at the International Symposium of the Society of Core Analysts, September 12-16, Trondheim, Norway.

Lager, A., Webb, K.J., Black, C.J.J. 2007. Impact of Brine Chemistry on Oil Recovery. Paper A24 presented at the 14th European Symposium on Improved Oil Recovery, 22 April, Cairo, Egypt.

Lake, L.W. 1989. Enhanced Oil Recovery, Prentice-Hall, Englewood Cliffs, NJ.

Lake, L. W., Bryant, S. L. and Araque-Martinez, A. N. 2002. Geochemistry and Fluid Flow, Elsevier Science B. V., Amsterdam, The Netherlands.

Lee, S.Y., Webb, K.J., Collins, I.R., Lager, A., Clarke, S.M., O'Sullivan M., Routh, A.F., Wang, X. 2010. Low Salinity Oil Recovery – Increasing Understanding of the Underlying Mechanisms. Paper SPE 129722 presented at the SPE Improved Oil recovery Symposium, 24-28 April, Tulsa, Oklahoma.

Ligthelm, D.J., Gronsveld, J., Hofman, J.P., Brussee, N.J., Marcelis, F., Van der Linde, H.A. 2009. Novel Waterflooding Strategy by Manipulation of Injection Brine Composition. Paper SPE 119835 presented at EUROPEC/EAGE Conference and Exhibition, 8-11 June, Amsterdam, The Netherlands.

Ma, S., Morrow, N. R., Xiaoyun, Z. 1997. Generalized Scaling of Spontaneous Imbibition Data for Strongly Water-Wet Systems. Journal of Petroleum Science and Engineering, **18** (3-4): 165-178.

Mattax, C.C. and Kyte, J.R. 1962. Imbibition Oil Recovery from Fractured, Water-Drive Reservoir. Paper SPE 187 SPE Journal **2** (2): 177-184.

McGuire, P.L., Chatam, J.R., Paskvan, F.K., Sommer, D.M., Carini, F.H. 2005. Low Salinity Oil Recovery: An Exciting New EOR Opportunity for Alaska's North Slope. Paper SPE 93903 presented at SPE Western Regional Meeting, 30 March – 1 April, Irvine, California.

Mohanty, K. K., Davis. H. T. and Scriven, L. E. 1987. Physics of Oil Entrapment in Water-Wet Rock. SPE Reservoir Engineering, **2** (1): 113-128.

Morrow, N.R. 1990. Wettability and its Effect on Oil Recovery. Journal of Petroleum technology, **42** (12): 1476-1484.

Oil & Gas Journal. 2012. 2012 Worldwide EOR Survey. http://www.ogj.com/articles/print/vol-110/issue-4/general-interest/special-report-eor-heavy-oil-survey/2012-worldwide-eor-survey.html

OPEC, 2013. OPEC Annual Statistical Bulletin, 2013; http://www.opec.org/library/Annual%20Statistical%20Bulletin/interactive/current/FileZ/XL/T31.HTM.

Peters, E. J. 2012. Advanced Petrophysics: Volume 2: Dispersion, Interfacial Phenomena/Wettability, Capillarity/Capillary Pressure, Relative Permeability. Austin, TX: Live Oak Book.

Pu, H., Xie, X., Yin, P., Morrow, N.R. 2008. Application of Coalbed Methane Water to Oil Recovery by Low Salinity Waterflooding. Paper SPE 113410 presented at SPE Improved Oil Recovery Symposium, 24-28 April, Tulsa, OK.

Puntervold, T. 2008. Waterflooding of Carbonate Reservoirs - EOR by Wettability Alteration. ISBN 978- 82-7644-347-9. PhD Dissertation.

Romanuka, J., Hofman, J.P., Ligthelm, D.J., Suijkerbuijk, B.M.J.M., Marcelis, A.H.M., Oedai, S., Brusee, N.J., van der Linde, H.A., Aksulu H., Austad, T. 2012. Low Salinity EOR in Carbonates. Paper SPE 153869 presented at the Eighteenth SPE Improved Oil Recovery Symposium, 14-18 April, Tulsa, OK.

Schechter, R. S. 1992. Oil Well Stimulation. Prentice Hall, Englewood Cliff, N.

Schechter, D. S., Zhou, D., and Orr, F. M. 1994. Low IFT and Drainage. Journal of Petroleum Science and Engineering, **11**: 283-300.

Schlumberger, 2007. Schlumberger Carbonate Reservoirs: Meeting Unique Challenges to Maximize Recovery; http://www.slb.com/~/media/Files/industry_challenges/carbonates/brochures/cb_carbonate_reservoirs_07os003.ashx.

Strand, S., Hognesen, E.J. and Austad, T. 2006. Wettability Alteration of Carbonates – Effects of Potential Determining Ions (Ca2+ and SO42-) and Temperature. Colloids and Surfaces A: Physicochemical Engineering Aspects **275** (1-3): 1-10.

Strand, S., Puntervold, T., and Austad, T. 2008. Effect of Temperature on Enhanced Oil Recovery from Mixed-wet Chalk Cores by Spontaneous Imbibition and Forced Displacement using Seawater. Energy & Fuels **22** (5): 3222–3225.

Tang, G.Q. and Morrow, N.R. 1997. Salinity, Temperature, Oil Composition, and Oil Recovery by Waterflooding. Journal Paper SPE 36680 SPE Reservoir Engineering **12** (4): 269–276.

Tang, G.Q. and Morrow, N.R. 1999. Influence of Brine Composition and Fines Migration on Crude Oil/Brine/Rock Interactions and Oil Recovery. Journal of Petroleum Science and Engineering **24** (2): 99–111.

Tang, G. and Morrow, N.R. 2002. Injection of Dilute Brine and Crude Oil/Brine/Rock Interactions. In Environmental Mechanics: Water, Mass and Energy Transfer in the Biosphere, **129**: 171-179.

Vo, L.T., Gupta, R., Hehmayer, O.J. 2012. Ion Chromatography Analysis of advanced Ion Management Carbonate Coreflood Experiments. Paper SPE 161821 presented at Abu Dhabi International Petroleum Exhibition & Conference, 11-14 November, Abu Dhabi, U.A.E.

Webb, K.J., Black, C.J.J., Al-Ajeel, H. 2004. Low Salinity Oil Recovery—Log-Inject-Log. Paper SPE 89379 presented at the SPE/DOE Symposium on Improved Oil Recovery, 17–21 April, Tulsa, OK.

Xie, X. and Morrow, N. R. 2000. Oil Recovery by Spontaneous Imbibition from Weakly Water-wet Rocks. Petrophysics, **42** (4): 313-322.

Yildiz, H.O. and Morrow, N.R. 1996. Effect of Brine Composition on Recovery Waterflooding of Moutray Crude Oil by Waterflood. Petroleum Science & Engineering, **14**: 159-168.

Yousef, A.A., Al-Saleh, S., Al-Jawfi, M. 2010. Laboratory Investigation of Novel Oil Recovery Method for Carbonate Reservoirs. Paper SPE 137634 presented at the SPE Canadian Unconventional Resources and International Petroleum Conference, 19-21 October, Calgary, Alberta, Canada.

Yousef, A.A., Al-Saleh, S., Al-Jawfi, M. 2012a. The Impact of the Injection Water Chemistry on Oil Recovery from Carbonate Reservoirs. Paper SPE 154077 presented at the SPE EOR Conference at Oil and Gas West Asia, 16-18 April, Muscat, Oman.

Yousef, A. A., Liu, L., Blanchard, G., Al-Saleh, S., Al-Zahrani, R., Al-Tammar, H. and Al-Mulhim, N. 2012b. Smartwater Flooding: Industry's First Field Test in Carbonate Reservoirs. Paper SPE 159526 presented at the SPE Annual Technical Conference and Exhibition, 8-10 October, San Antonia, TX.

Zaretskiy, Y. 2012. Towards modeling Physical and Chemical Effects During Wettability Alteration in Carbonates at Pore and Continuum Scale. PhD dissertation.

Zhang, Y. and Sarma H. 2012. Improving Waterflood Recovery Efficiency in Carbonate Reservoirs through Salinity Variations and Ionic Exchanges: A Promising Low-Cost "Smart-Waterflood" Approach. Paper SPE 141631 presented at the Abu Dhabi International Petroleum Exhibition & Conference, 11-14 November, Abu Dhabi, U.A.E.

Zhang, P. and Austad, T. 2005. Waterflooding in Chalk: Relationship between Oil Recovery, New Wettability Index, Brine Composition and Cationic Wettability Modifier. Paper SPE 94209 presented at the SPE Europec/EAGE Annual Conference, 13-16 June, Madrid, Spain.

Zhang, P., Tweheyo, M.T., Austad, T. 2007. Wettability Alteration and Improved Oil Recovery by Spontaneous Imbibition of Seawater into Chalk: Impact of the Potential Determining Ions Ca2+, Mg2+, and SO42-. Colloids and Surfaces A: Physicochem. Eng. Aspects **301**: 199–208.